NACA RM L50B13

NACA

RESEARCH MEMORANDUM

INVESTIGATION AT HIGH SUBSONIC SPEEDS OF A 45° SWEPTBACK HORIZONTAL TAIL WITH PLAIN AND HORN-BALANCED CONTROL SURFACES

By Harold S. Johnson and Robert F. Thompson

Langley Aeronautical Laboratory
Langley Air Force Base, Va.

NATIONAL ADVISORY COMMITTEE
FOR AERONAUTICS
WASHINGTON

March 31, 1950
Declassified July 29, 1954

NACA RM L50B13

NATIONAL ADVISORY COMMITTEE FOR AERONAUTICS

RESEARCH MEMORANDUM

INVESTIGATION AT HIGH SUBSONIC SPEEDS OF A 45° SWEPTBACK HORIZONTAL TAIL WITH PLAIN AND HORN-BALANCED CONTROL SURFACES

By Harold S. Johnson and Robert F. Thompson

SUMMARY

An investigation was made in the Langley high-speed 7- by 10-foot tunnel of the aerodynamic and hinge-moment characteristics of an untapered, aspect ratio 3, semispan horizontal-tail model having 45° of sweepback through a Mach number range of from 0.50 to about 0.89. The model was equipped with an unbalanced and a horn-balanced 25-percent-chord elevator. A comparison is made with the results of a previous investigation of the same model equipped with a larger horn balance.

The investigation showed that the incremental rate of change of hinge-moment coefficient with angle of attack and with elevator deflection C_{h_α} and C_{h_δ} due to the horn balance became more positive with increasing horn size and was relatively unaffected by Mach number variations for the speed range covered in the investigation. For a given change in horn size, C_{h_δ} changed approximately 3.5 times as much as C_{h_α}.

The horn-balanced elevator tested appeared to offer satisfactory hinge-moment characteristics for the Mach number range investigated.

INTRODUCTION

The necessity of providing a means of reducing the high-speed control forces of the faster, more heavily loaded airplanes currently in use or being designed while retaining sufficient control for landing and take-off has presented a problem to airplane designers. Even though a control system incorporates a power boost, it is desirable to balance aerodynamically a large part of the control force. It has been found that the use of a horn balance is one method of reducing the aerodynamic hinge moments at low speeds (references 1 to 4). In addition, the horn

type of balance provides a convenient attachment for counterbalances to statically balance the control. In order to provide additional information on the characteristics of balanced control surfaces suitable up to high subsonic speeds, a series of investigations are being conducted in the Langley 7- by 10-foot tunnels.

The data presented and discussed herein are the results of an investigation of the aerodynamic and hinge-moment characteristics of an untapered, aspect ratio 3, semispan horizontal-tail model having 45° of sweepback and an NACA 0012 airfoil section perpendicular to the leading edge. The model was equipped with an unbalanced and a horn-balanced 25-percent-chord elevator and was tested through a speed range to a Mach number of about 0.89. The present investigation is an extension of the investigation reported in reference 5. The model used in the present investigation and that reported in reference 5 were essentially the same, differing only in horn-balance size. Reference 5 presents data for three sizes of horn balance and the effects of fairing the horn inboard edge (edge normal to the hinge axis) at low speed (M = 0.30) in addition to data through a Mach number range for the model equipped with a larger horn balance than the horn tested in the present investigation.

MODEL AND APPARATUS

The semispan horizontal-tail model used for the investigation had an NACA 0012 airfoil section perpendicular to the leading edge (14.65° trailing-edge angle), an aspect ratio of 3.00 (based on the full-span dimensions), a taper ratio of 1, 45° of sweepback, and was equipped with a $0.25\bar{c}$ unsealed elevator with a radius elevator nose. The model was constructed of hardened steel to the plan form indicated in figure 1. The elevator was tested with and without a horn balance. (See fig. 2.) The horn balance, referred to in the text and in the figures as the small horn, was triangular in shape and the horn inboard edge was perpendicular to the elevator hinge axis. The intermediate horn as shown in figure 2 was tested in a previous investigation (reference 5). The inboard edges of the horns were faired (fig. 2). The dimensional characteristics of the two horn balances are presented in table I. A $\frac{1}{16}$-inch gap was maintained between the horn inboard edge and the stabilizer.

Structural calculations indicated that more than two hinges would be necessary. Reference 6 indicates that for control surfaces having three hinges, the hinge-moment increments resulting from distortion can be an appreciable fraction of the total hinge moment. In order to avoid the inclusion of such hinge-moment increments, the elevator was constructed in two spanwise segments. The $\frac{1}{16}$-inch gap between the

two halves was unsealed. The elevator hinge-moments were measured by calibrated beam-type electrical strain gages mounted within the stabilizer. The total hinge moment of the semispan elevator was the summation of the hinge moments of the two spanwise segments. The elevator deflections were varied by changing the strain-gage yokes attached to the elevator.

The semispan model was mounted vertically in the Langley high-speed 7- by 10-foot tunnel as shown in figure 3 with the root chord adjacent to the tunnel ceiling which thereby acted as a reflection plane. The model was supported entirely by the balance frame so that all forces and moments acting on the model could be measured. A small clearance was maintained between the model and the tunnel ceiling. A metal end plate was attached to the model at the root chord to deflect the air flowing into the test section through the clearance hole in order to minimize the effect of this air flow on the flow over the model. Provisions were made for changing the angle of attack of the model while the tunnel was in operation.

COEFFICIENTS AND SYMBOLS

C_L	lift coefficient (L/qS)
C_D	drag coefficient (D/qS)
C_m	pitching moment ($M^l/qS\bar{c}$)
C_h	elevator hinge-moment coefficient ($H/qb_1\bar{c}_e^2$)
L	twice lift of semispan model, pounds
D	twice drag of semispan model, pounds
M^l	twice pitching moment of semispan model measured about the aerodynamic center at M = 0.30 (1.63 ft behind root-chord leading edge), foot-pounds
H	twice hinge moment of semispan model elevator measured about the elevator hinge line, foot-pounds
S	twice area of semispan model, 9.21 square feet
S_e	area of semispan model elevator behind hinge line, 1.15 square feet
S_H	area of model horn, square feet (see table I)
b	twice span of semispan model, 5.26 feet

b_l twice span of semispan elevator measured along hinge line, feet

$\bar{c}$ mean aerodynamic chord, 1.77 feet

$\bar{c}_e$ root-mean-square chord of model elevator behind hinge line (measured perpendicular to hinge line), 0.31 foot

c_e average chord of model elevator behind hinge line (measured perpendicular to hinge line), 0.31 foot

c_H average chord of model horn (measured perpendicular to hinge line), feet (see table I)

B balance coefficient $\left(\sqrt{S_H c_H / S_e c_e}\right)$

α angle of attack of model chord plane, degrees

δ_e elevator deflection relative to stabilizer, measured normal to the elevator hinge line (positive when trailing edge is down), degrees

M Mach number (V/a)

V free-stream velocity, feet per second

a speed of sound, feet per second

q free-stream dynamic pressure, pounds per square foot $\left(\frac{1}{2}\rho V^2\right)$

ρ mass density of air, slugs per cubic foot

$$C_{h_\alpha} = \left(\frac{dC_h}{d\alpha}\right)_{\delta_e}$$

$$C_{h_\delta} = \left(\frac{dC_h}{d\delta}\right)_{\alpha}$$

$$C_{L_\alpha} = \left(\frac{dC_L}{d\alpha}\right)_{\delta_e}$$

$$C_{L_\delta} = \left(\frac{dC_L}{d\delta}\right)_{\alpha}$$

$\alpha_\delta = \left(\frac{C_{L_\delta}}{C_{L_\alpha}}\right)$

ΔC_{h_α} C_{h_α} of elevator with horn balance minus C_{h_α} of elevator without horn balance

ΔC_{h_δ} C_{h_δ} of elevator with horn balance minus C_{h_δ} of elevator without horn balance

The subscripts outside the parentheses indicate the factors held constant during the measurement of the parameters. The slopes were measured in the vicinity of $\alpha = 0^\circ$ and $\delta_e = 0^\circ$.

CORRECTIONS

Jet-boundary corrections were computed by the method of reference 7, using values of boundary-induced upwash computed for swept wings from reference 8. The corrections were applied to the angles of attack and to the drag-coefficient data in accordance with the following equations:

$$\alpha = \alpha_M + 0.553C_{L_M}$$

$$C_D = C_{D_M} + 0.0083C_{L_M}^2$$

where the subscript M indicates measured values. The jet-boundary corrections to the lift, pitching-moment, and hinge-moment data were considered negligible and therefore were not applied.

All coefficients and Mach numbers were corrected for blocking by the model and its wake. The blockage corrections were computed by the methods presented in reference 9.

Based on calculations and tests of other models of similar construction, the deflection of the model under load is believed to have been small and, therefore, to have a negligible effect on the aerodynamic characteristics of the model. A calibration test indicated that corrections to the elevator angle due to deflection under load at $\alpha = 0^\circ$ were negligible for the range of elevator angles investigated. No attempt was made to correct for the air flow through the gap at the root of the model or between the two elevator segments.

TESTS AND TEST CONDITIONS

For the model equipped with the small faired horn and with the plain elevator, test data were obtained at four values of elevator deflection (0°, -1.7°, -3.7°, and -7.8°) and at six values of Mach number covering a range from 0.50 to about 0.89. The tests were made through a $\pm 16^\circ$ angle-of-attack range for the horn-balance elevator and a $\pm 8^\circ$ range for the plain elevator except for conditions where tunnel power limitations restricted the angle-of-attack range.

The variation of test Reynolds number with Mach number for average test conditions is presented as figure 4. The Reynolds numbers are based on the mean aerodynamic chord (1.77 ft).

RESULTS AND DISCUSSION

Presentation of Data

The variations of the aerodynamic coefficients C_L, C_D, C_m, and C_h with angle of attack through the speed range up to a Mach number of about 0.89 are presented as figures 5 to 10 for the model equipped with the elevator having the small horn balance and as figures 11 to 16 for the model equipped with the plain elevator. The hinge-moment coefficients presented are for the complete elevator. The variations of the hinge-moment parameters C_{h_α} and C_{h_δ} with Mach number for the plain elevator, the elevator with the small horn balance, and the elevator with the intermediate horn balance (from reference 5) are shown in figure 17. Incremental values of the hinge-moment parameters due to the horn balances are presented in figure 18. The effects of Mach number on the lift parameters C_{L_α}, C_{L_δ}, and α_δ are presented in figure 19.

Hinge-Moment Characteristics

The control hinge-moment parameter C_{h_α}, for the elevator equipped with either the small or the intermediate horn or with no horn balance, became less negative or more positive with increasing Mach number and this increase became more rapid for Mach numbers greater than about 0.82 (fig. 17). The elevator equipped with the intermediate horn balance ($B = 0.36$) had a small positive value of C_{h_α} (or against the relative wind floating tendency) at the lowest speed investigated ($M = 0.5$) and C_{h_α} became more positive as the Mach number was increased (from reference 5). Reducing the balance coefficient by changing from

the intermediate to the small horn (B = 0.28) displaced the curve in a negative direction so that C_{h_α} was positive only above a Mach number of about 0.72. The parameter C_{h_α} for the model equipped with the plain elevator was negative throughout the speed range and approached zero at the highest test Mach number (M = 0.89). The effects of Mach number on the increments of C_{h_α} due to the horn balances are shown in figure 18. In agreement with the data of reference 2, ΔC_{h_α} increased with increasing horn size. The increment increased slightly with Mach number for both horn balances tested.

For the three model configurations, the hinge-moment parameter C_{h_δ} increased fairly linearly with increasing Mach number to a Mach number of about 0.82; above this speed C_{h_δ} increased more rapidly with increases in Mach number (fig. 17). The intermediate horn-balanced elevator (from reference 5) was overbalanced (positive C_{h_δ}) for Mach numbers greater than about 0.63. Reducing the horn size to that of the small horn balance eliminated the overbalancing tendency, although C_{h_δ} was only slightly negative at the highest Mach number attained in the investigation. As expected, the increment of C_{h_δ} due to the horn balance increased as the horn size was increased (fig. 18). Figure 18 also shows that the balancing effectiveness of the horn increased slightly as the Mach number was increased and the increase was more pronounced for the larger horn. As noted in reference 5, a study of the hinge-moment characteristics of the inboard and outboard portions of the elevator (data not presented) showed that the values of C_{h_δ} for the inboard segment of the elevator did not vary with Mach number. The additional data of this investigation show that most of the positive increase in the values of C_{h_δ} with Mach number, as discussed in reference 5, can now be attributed to a reduction in hige moment of the outboard segment of the unbalanced elevator and that the increase in balancing power of the horn with Mach number accounts for only a small part of the variation of C_{h_δ} with M.

A study of figures 5 to 16 and the data of reference 5 reveals that both C_{h_α} and C_{h_δ} generally became more negative as the angle of attack is varied from $\alpha = 0^\circ$.

For a given change in horn size, the data of figures 17 and 18 show that C_{h_δ} changes about 3.5 times as much as C_{h_α}. This change is much larger than that for the horn balance on unswept surfaces where the ratio was more nearly 1 (references 2 and 4).

The small horn-balanced elevator appeared to offer satisfactory control characteristics throughout the speed range investigated provided that the small positive values of C_{h_α} at the higher Mach numbers can be tolerated. References 10 and 11 show that the trailing-edge angle has a marked effect on the hinge-moment characteristics at high speeds and recommend that the trailing-edge angle be kept to a minimum, preferably below 14° (measured perpendicular to the elevator hinge line). Decreasing the trailing-edge angle generally eliminates the positive increase in both C_{h_α} and C_{h_δ} with increases in M and, for some configurations with small trailing-edge angles, a negative increase in the hinge-moment parameters with Mach number is shown (reference 12, 8° trailing-edge angle). The low-speed values of both C_{h_α} and C_{h_δ} are also increased negatively when the trailing-edge angle is decreased. The trailing-edge angle of the model used in the present investigation was 14.65°. It is therefore believed that the hinge-moment characteristics of this model would be improved by reducing the trailing-edge angle, and that the horn balance is a satisfactory device for obtaining desirable control characteristics for sweptback control surfaces for the speed range investigated.

The data of references 4 and 5 show that fairing the inboard or leading edge of the horn balance has a pronounced unbalancing effect (negative increase in C_{h_δ}) with little or no effect on C_{h_α}, and thus the designer is provided with a powerful tool for adjusting the balancing characteristics of a horn-balanced control surface once a satisfactory rate of change of hinge-moment coefficient with angle of attack is obtained.

Other Aerodynamic Characteristics

The rate of change of lift coefficient with angle of attack C_{L_α} increased with Mach number, and, for the Mach number range tested, the rate of increase of C_{L_α} with M was more rapid at the higher Mach numbers (fig. 19). As expected, C_{L_α} was unaffected by the horn or by changes in horn size. The addition of the horn balances slightly increased the values of C_{L_δ}. The parameter C_{L_δ} also increased as the horn size was increased.

For the three elevator configurations tested, C_{L_δ} did not vary with Mach number for the speed range investigated. Because of the aforementioned changes in C_{L_α} and C_{L_δ} with M and horn-balance area, respectively, the elevator effectiveness α_δ decreased with increasing Mach number and increased with increasing horn area. The small numerical increases in in C_{L_δ} and α_δ are attributed to the increased area of the elevator contributed by the horn balance.

A more complete discussion of the lift characteristics and a discussion of the drag characteristics of the model are presented in reference 5.

CONCLUSIONS

The results of the investigation of a 45° sweptback horizontal tail with plain and horn-balanced control surfaces indicated the following conclusions:

1. The incremental rate of change of hinge-moment coefficient with angle of attack and with elevator deflection C_{h_α} and C_{h_δ} due to the horn balance became more positive with increasing horn size and was relatively unaffected by Mach number variations for the range covered in the investigation. The hinge-moment parameters for the plain elevator became less negative with increasing Mach number.

2. For a given change in horn size, C_{h_δ} changed approximately 3.5 times as much as C_{h_α}.

3. The horn-balanced elevator tested appeared to offer satisfactory hinge-moment characteristics for the speed range covered in the investigation provided that the slight positive values of the rate of change of hinge-moment coefficient with angle of attack at the higher speeds is acceptable. A decrease in the elevator trailing-edge angle should result in an improvement in the variation of the hinge-moment characteristics with Mach number.

4. The rate of change of lift coefficient with angle of attack C_{L_α} increased with Mach number and was unaffected by either the presence of the horn or changes in horn size. The rate of change of lift coefficient with elevator deflection C_{L_δ} did not vary with Mach number but increased with increases in horn size. The elevator effectiveness parameter α_δ decreased with increasing Mach number and increased with increasing horn size.

Langley Aeronautical Laboratory
National Advisory Committee for Aeronautics
Langley Air Force Base, Va.

REFERENCES

1. Cleary, Joseph W., and Krumm, Walter J.: High-Speed Aerodynamic Characteristics of Horn and Overhang Balances on a Full-Scale Elevator. NACA RM A7H29, 1948.

2. Lowry, John G.: Résumé of Hinge-Moment Data for Unshielded Horn-Balanced Control Surfaces. NACA RB 3F19, 1943.

3. Thomas, H. H. B. M., and Lofts, M.: Analysis of Wind Tunnel Data on Horn Balance. Rep. No. Aero. 1994, British R.A.E., Nov. 1944.

4. Lowry, John G., Maloney, James A., and Garner, I. Elizabeth: Wind-Tunnel Investigation of Shielded Horn Balances and Tabs on a 0.7-Scale Model of XF6F Vertical Tail Surface. NACA ACR 4C11, 1944.

5. Johnson, Harold S., and Thompson, Robert F.: Investigation of Horn Balances on a 45° Sweptback Horizontal Tail Surface at High Subsonic Speeds. NACA RM L8J01, 1948.

6. Becker, John V., and Cooper, Morton: Structural Hinge-Moment Increments Caused by Hinge-Axis Distortion. NACA TN 1038, 1946.

7. Swanson, Robert S., and Toll, Thomas A.: Jet-Boundary Corrections for Reflection-Plane Models in Rectangular Wind Tunnels. NACA Rep. 770, 1943.

8. Polhamus, Edward C.: Jet-Boundary-Induced-Upwash Velocities for Swept Reflection-Plane Models Mounted Vertically in 7- by 10-Foot, Closed, Rectangular Wind Tunnels. NACA TN 1752, 1948.

9. Herriot, John G.: Blockage Corrections for Three-Dimensional-Flow Closed-Throat Wind-Tunnels, with Consideration of the Effect of Compressibility. NACA RM A7B28, 1947.

10. Lowry, John G., Axelson, John A., and Johnson, Harold I.: Effects of Sweep on Controls. NACA RM L8A28c, 1948.

11. Axelson, John A.: A Summary and Analysis of Wind-Tunnel Data on the Lift and Hinge-Moment Characteristics of Control Surfaces up to a Mach Number of 0.90. NACA RM A7L02, 1947.

12. Johnson, Harold I.: Measurements of Aerodynamic Characteristics of a 35° Sweptback NACA 65-009 Airfoil Model with $\frac{1}{4}$-Chord Plain Flap by the NACA Wing-Flow Method. NACA RM L7F13, 1947.

TABLE I.- HORN DIMENSIONS

Horn	Horn span (in.) (a)	Average chord (in.) (b)	Area, (sq in.)	Balance coefficient, B
Intermediate	6.42	3.53	22.66	0.36
Small	5.42	2.99	16.20	.28

[a]Measured parallel to hinge line.

[b]Measured normal to hinge line.

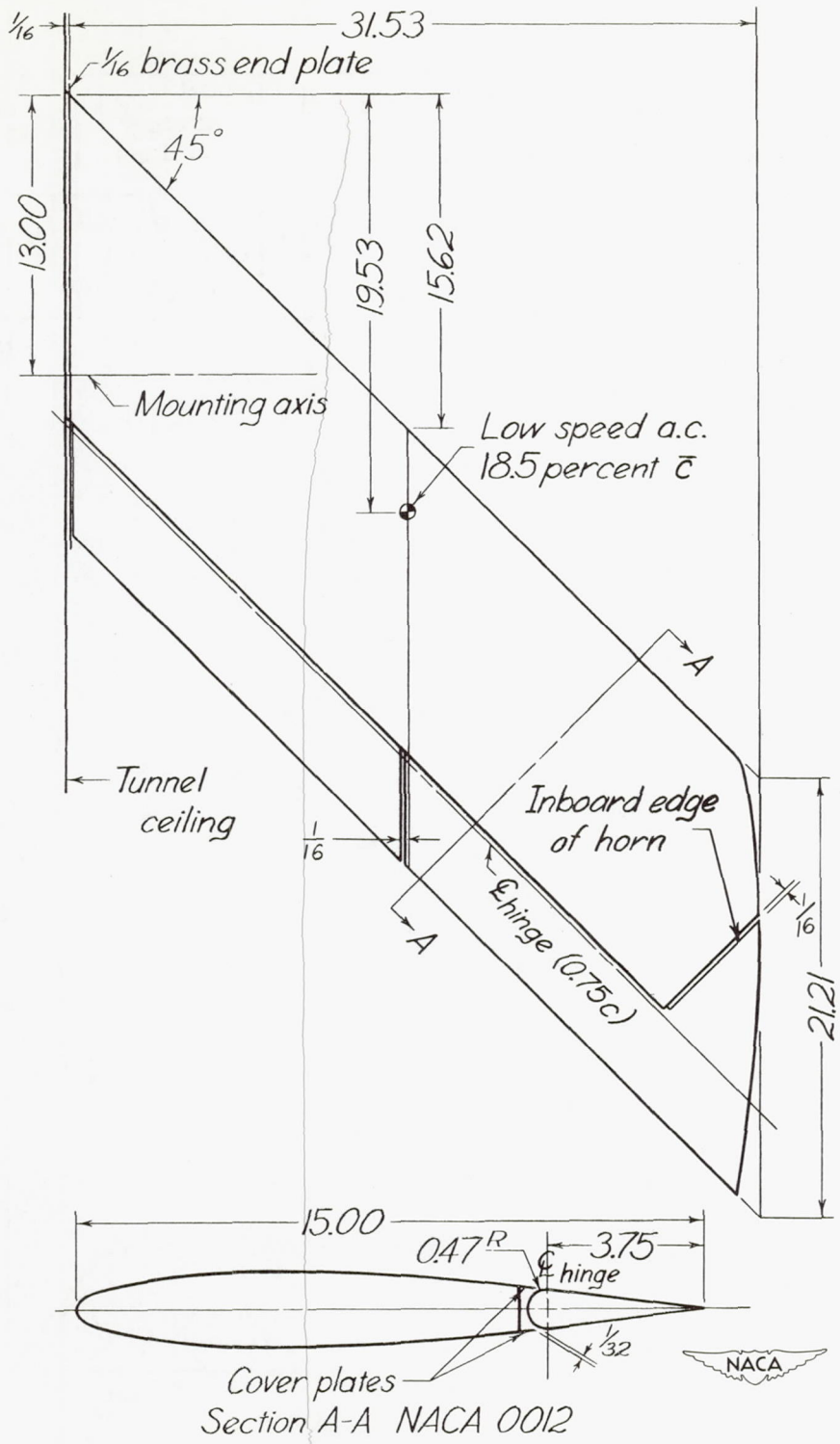


Figure 1.- Drawing of the 45° sweptback semispan horizontal-tail model equipped with the small horn. (All dimensions are in inches.)

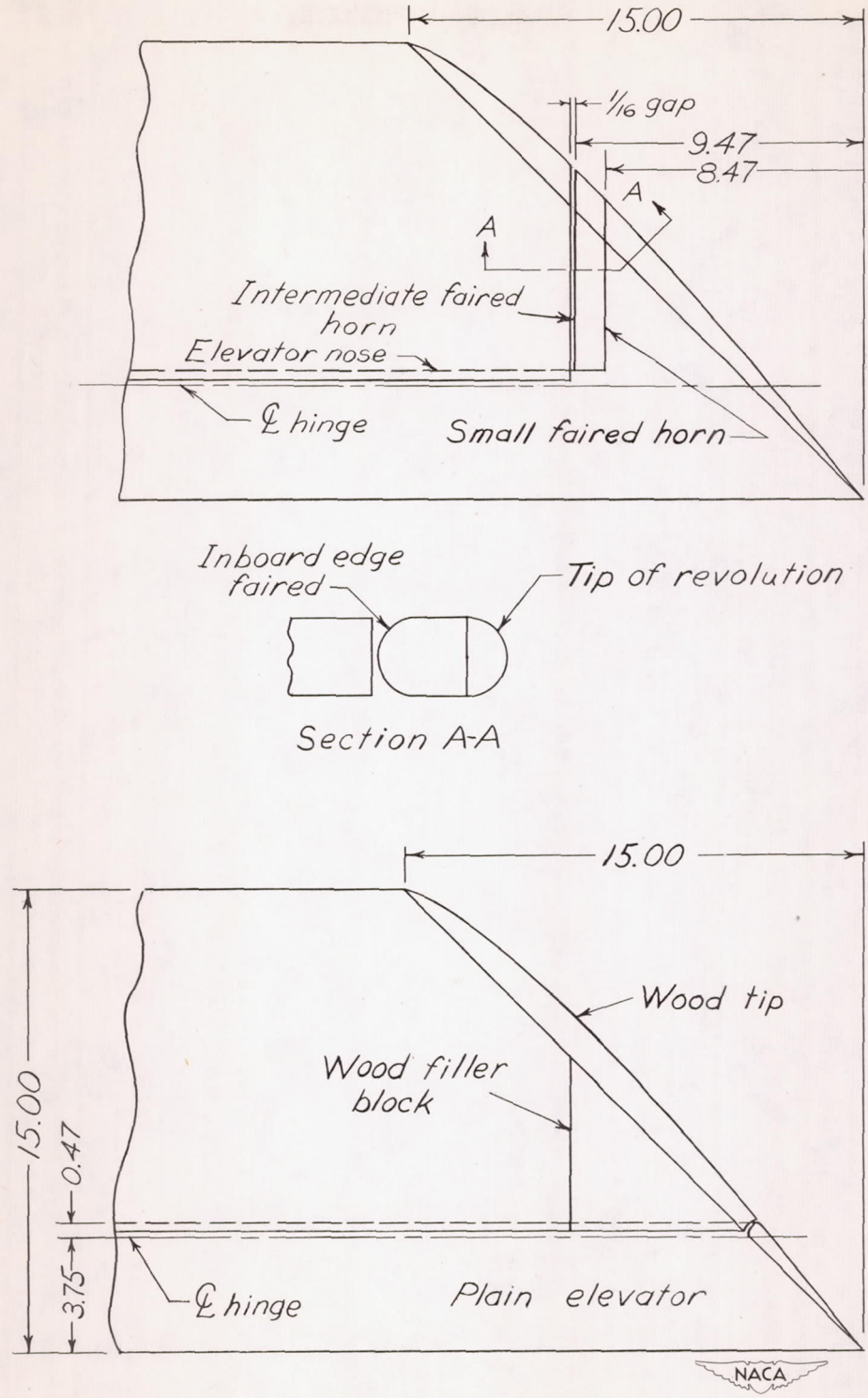


Figure 2.- Dimensions of the horn balances and plain elevator used for tests of the 45° sweptback horizontal-tail model. (All dimensions are in inches.)

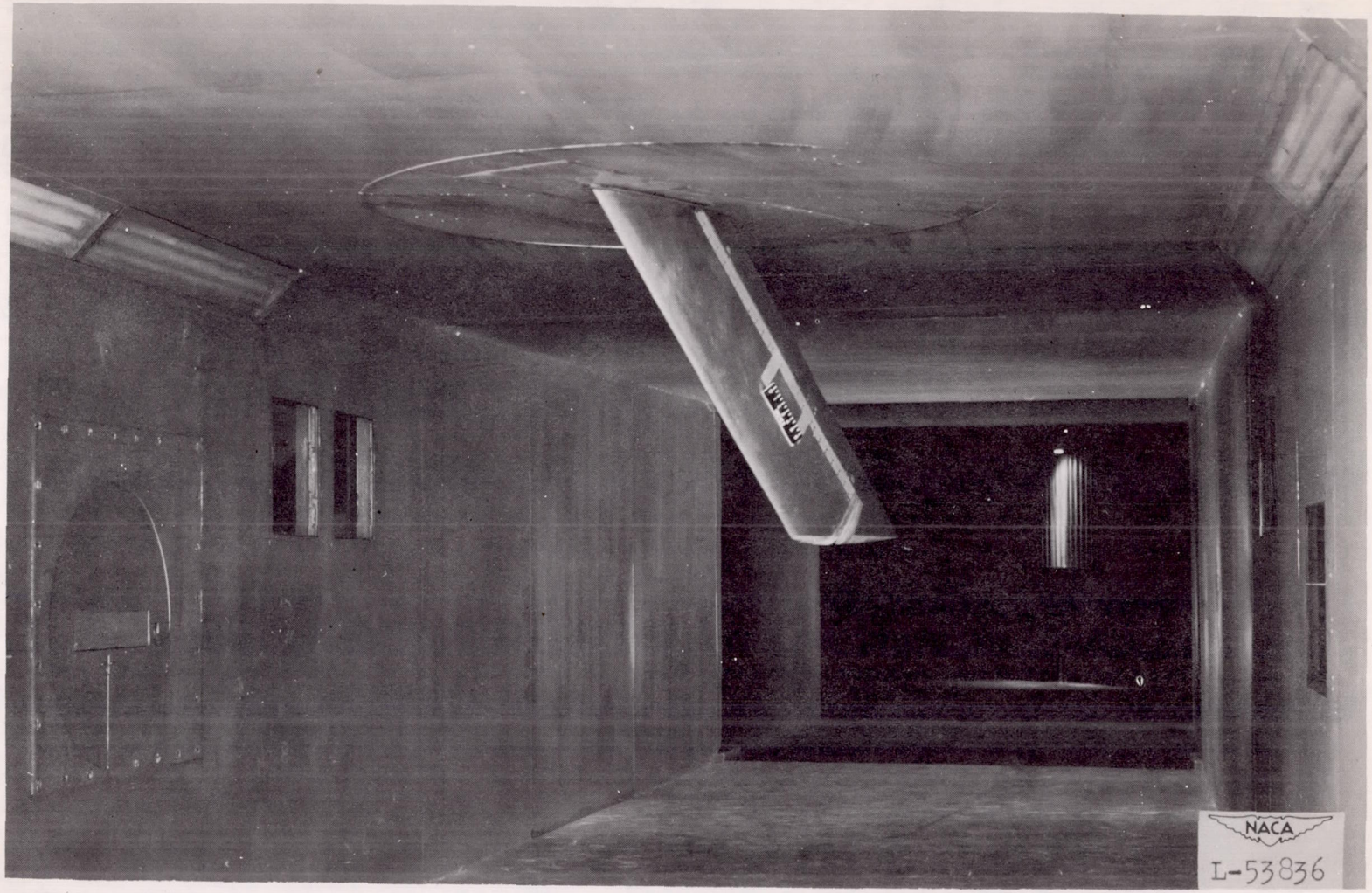


Figure 3.- The 45° sweptback horizontal-tail model mounted in the Langley high-speed 7- by 10-foot tunnel.

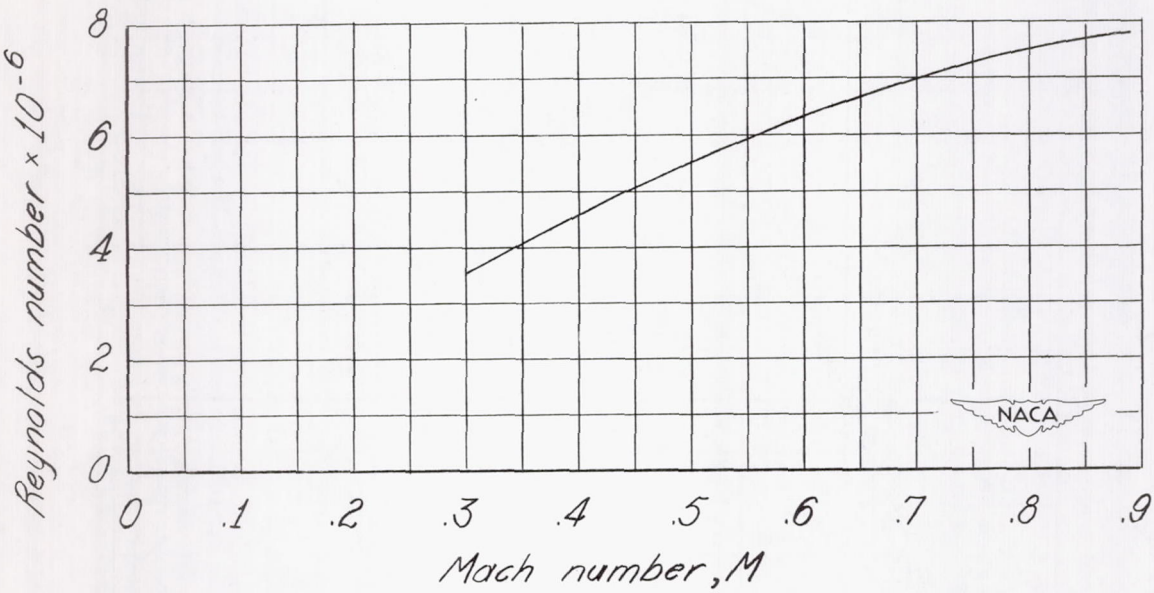


Figure 4.- Variation of average Reynolds number with Mach number.

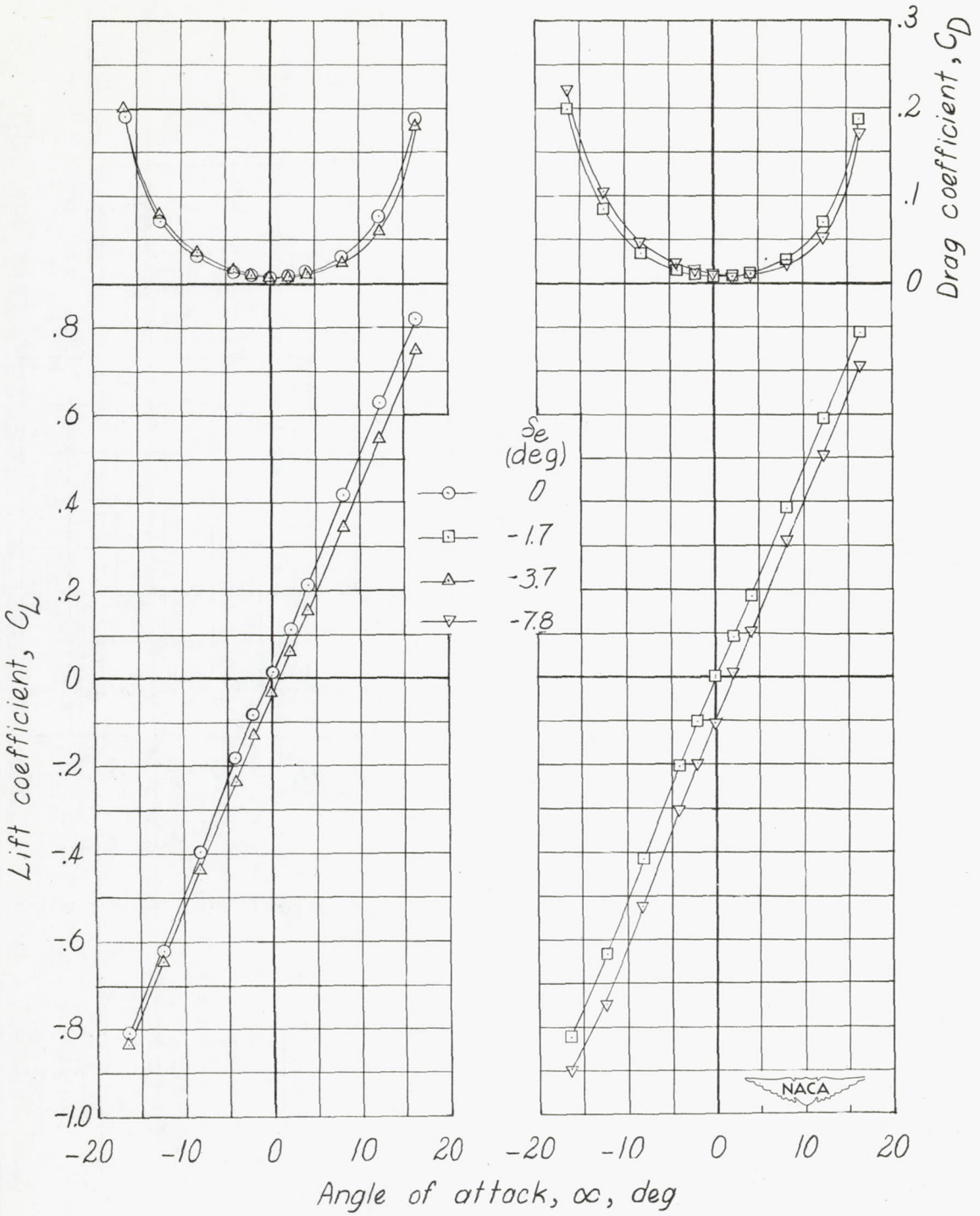


Figure 5.- Aerodynamic characteristics of the 45° sweptback horizontal-tail model equipped with the small faired horn. M = 0.50.

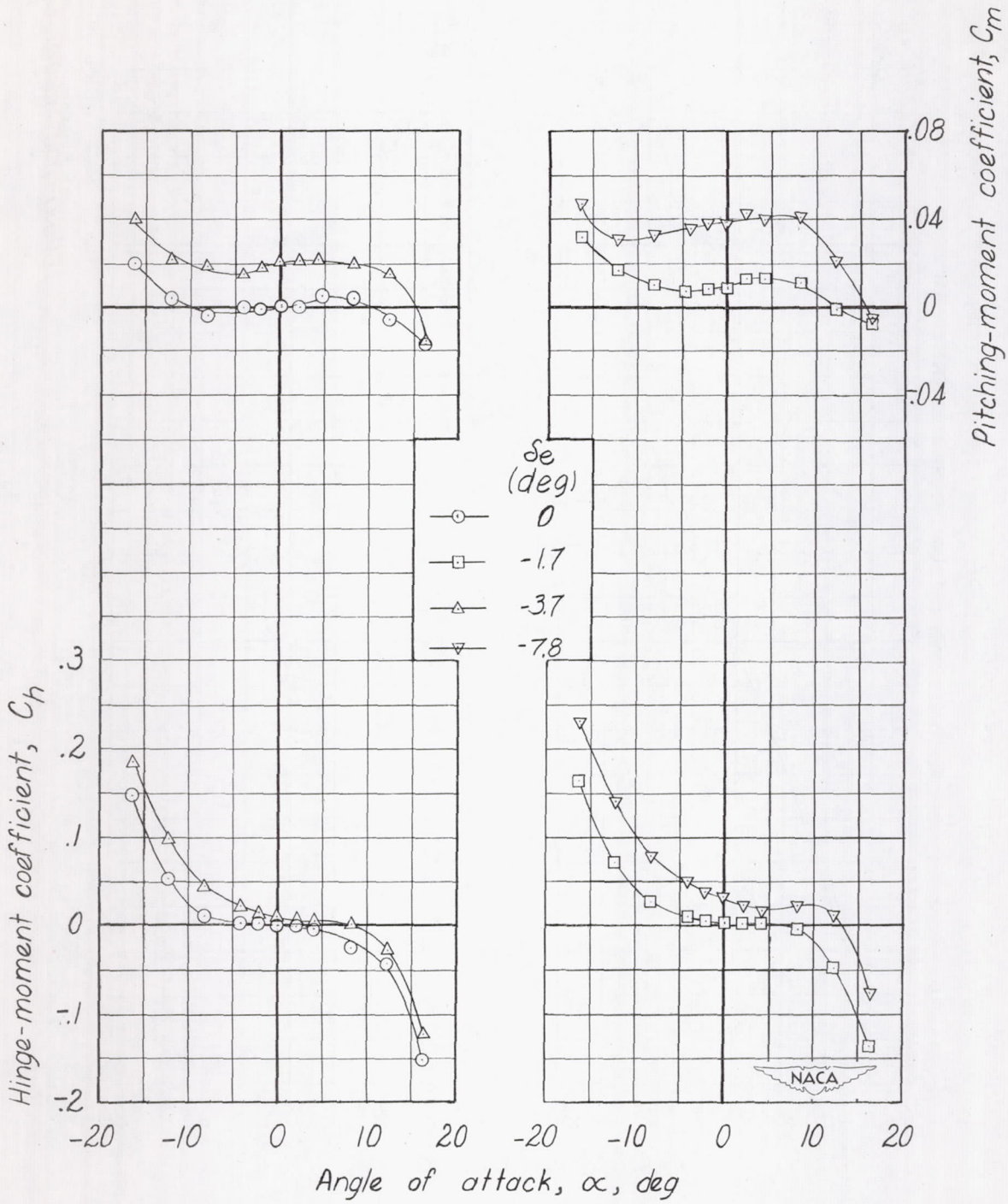


Figure 5.- Concluded.

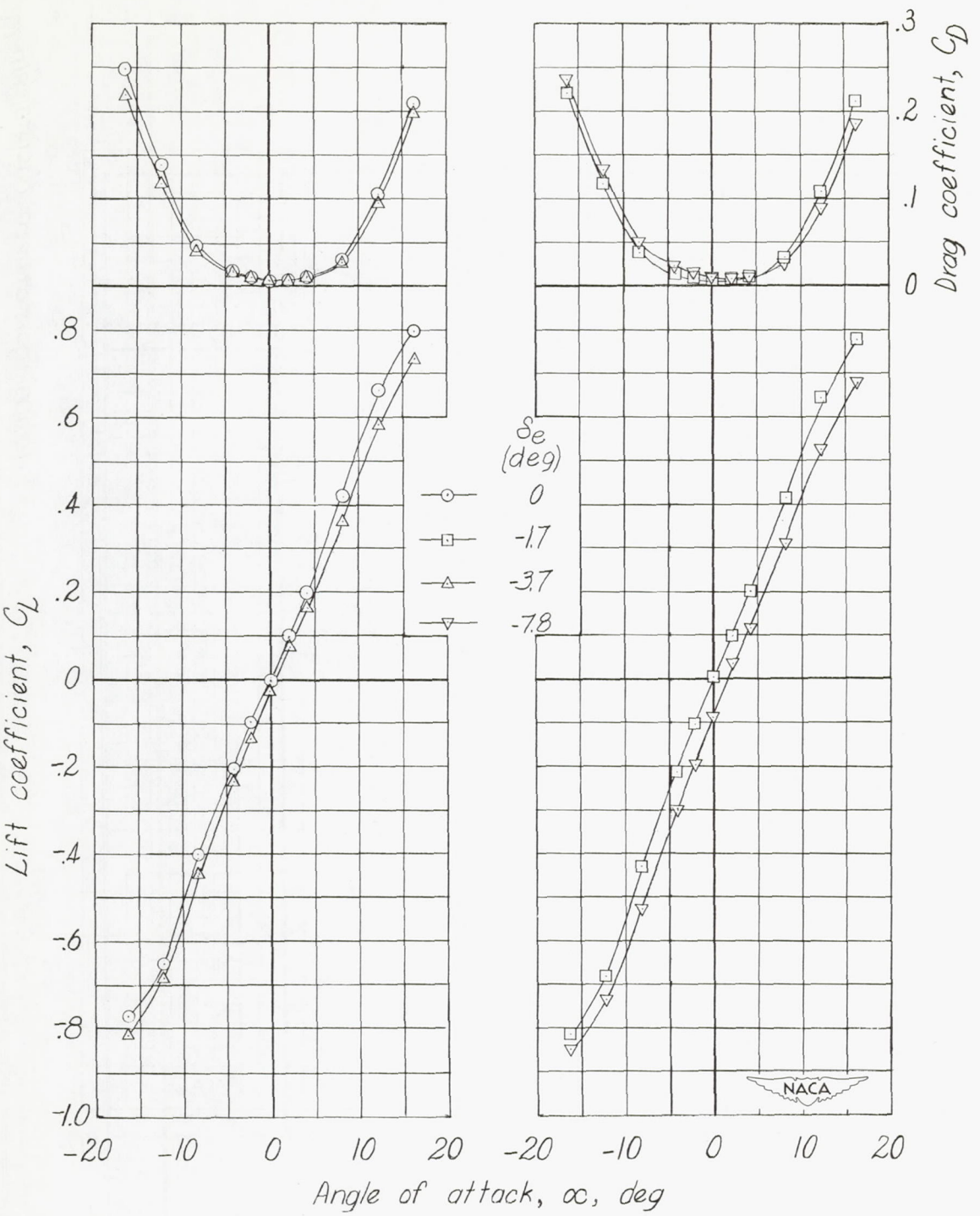


Figure 6.- Aerodynamic characteristics of the 45° sweptback horizontal-tail model equipped with the small faired horn. M = 0.70.

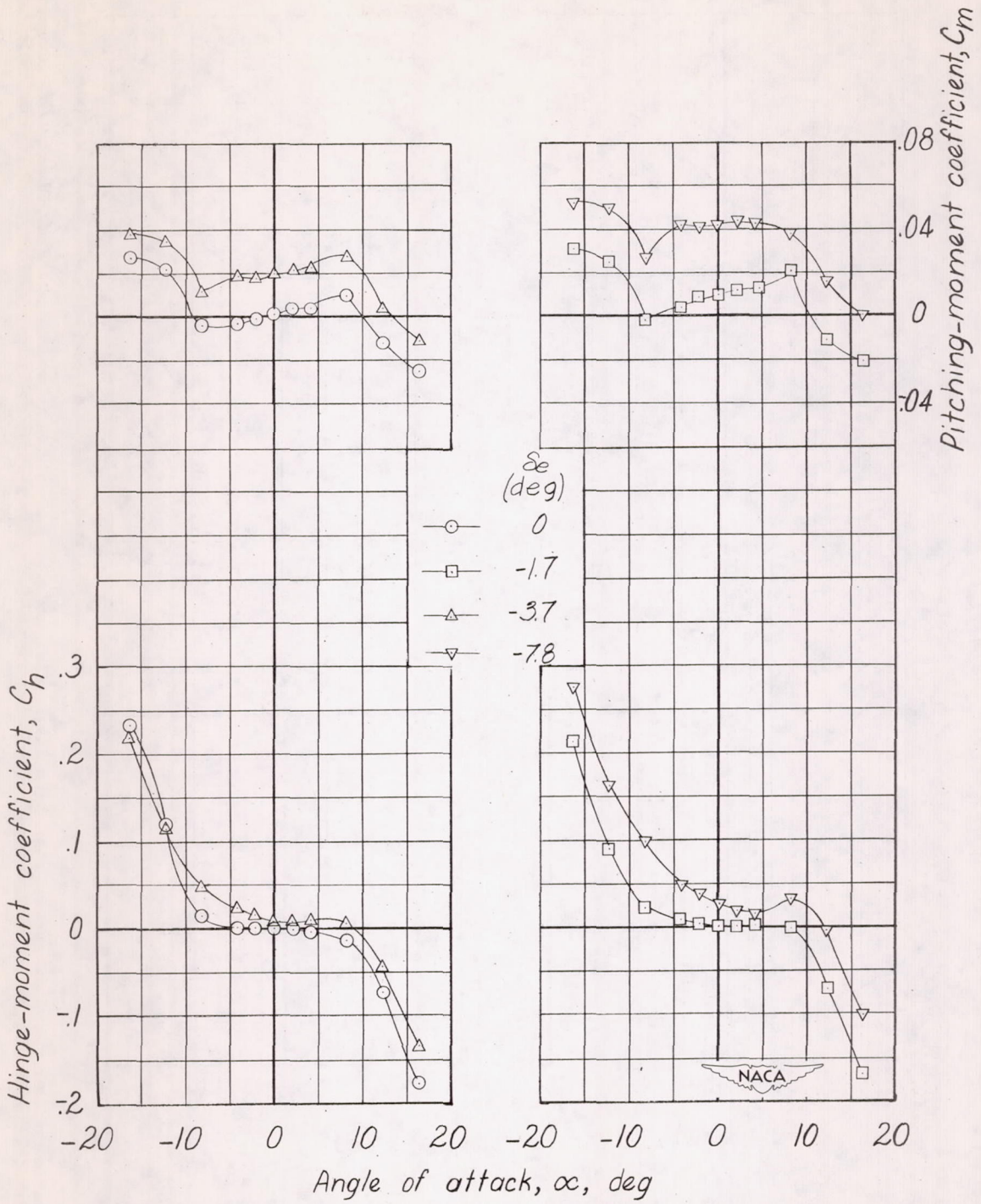


Figure 6.- Concluded.

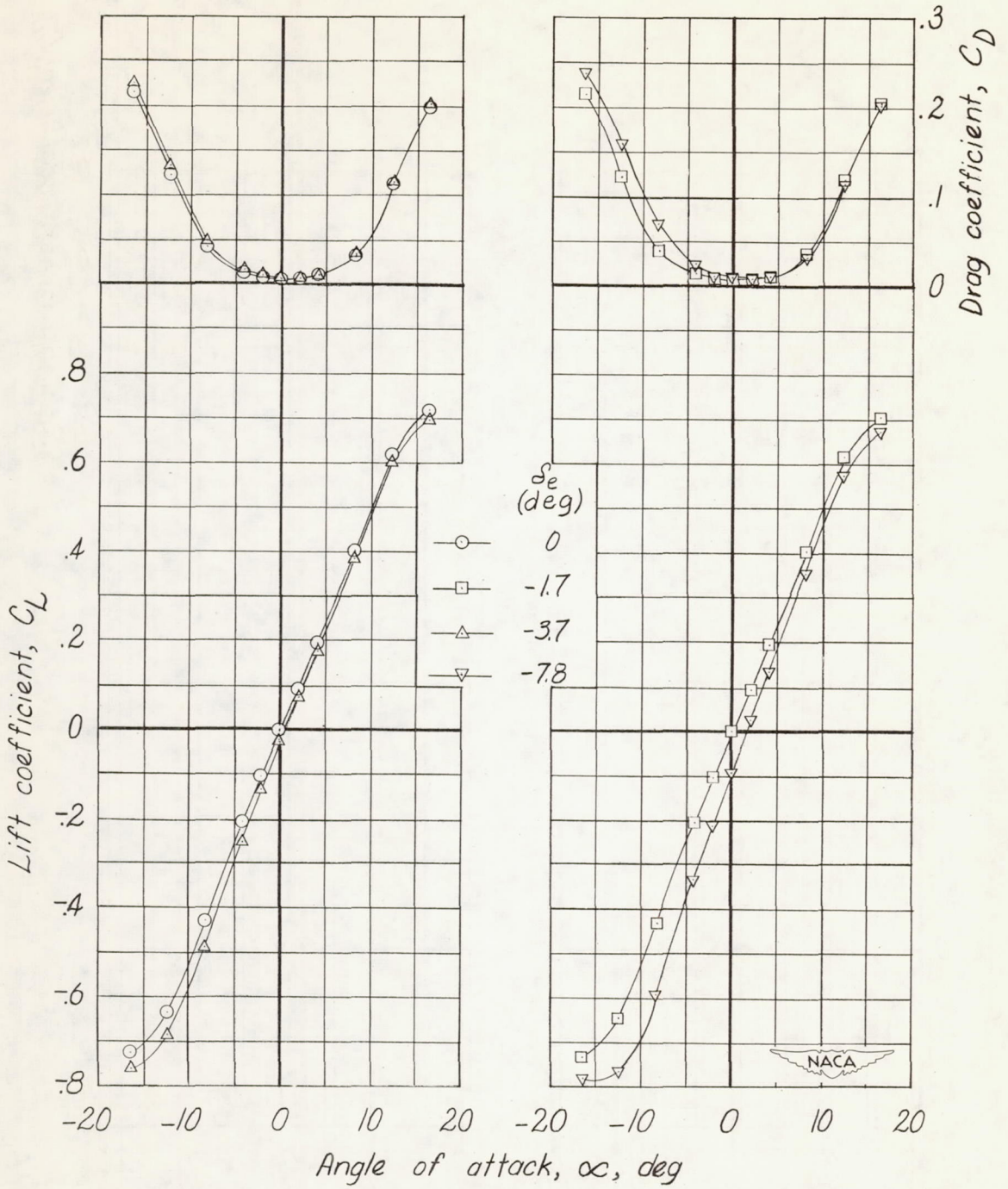


Figure 7.- Aerodynamic characteristics of the 45° sweptback horizontal-tail model equipped with the small faired horn. M = 0.81.

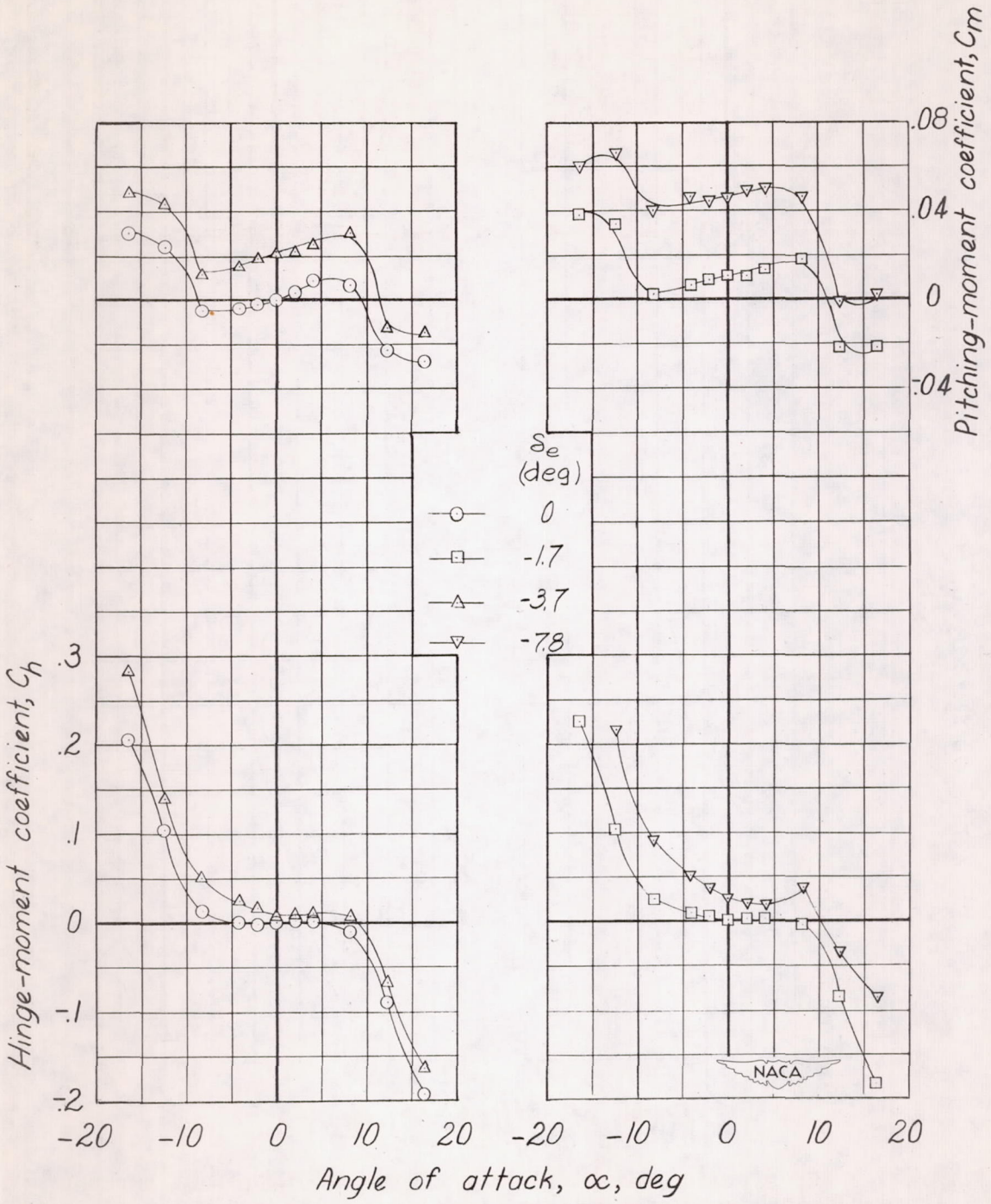


Figure 7.- Concluded.

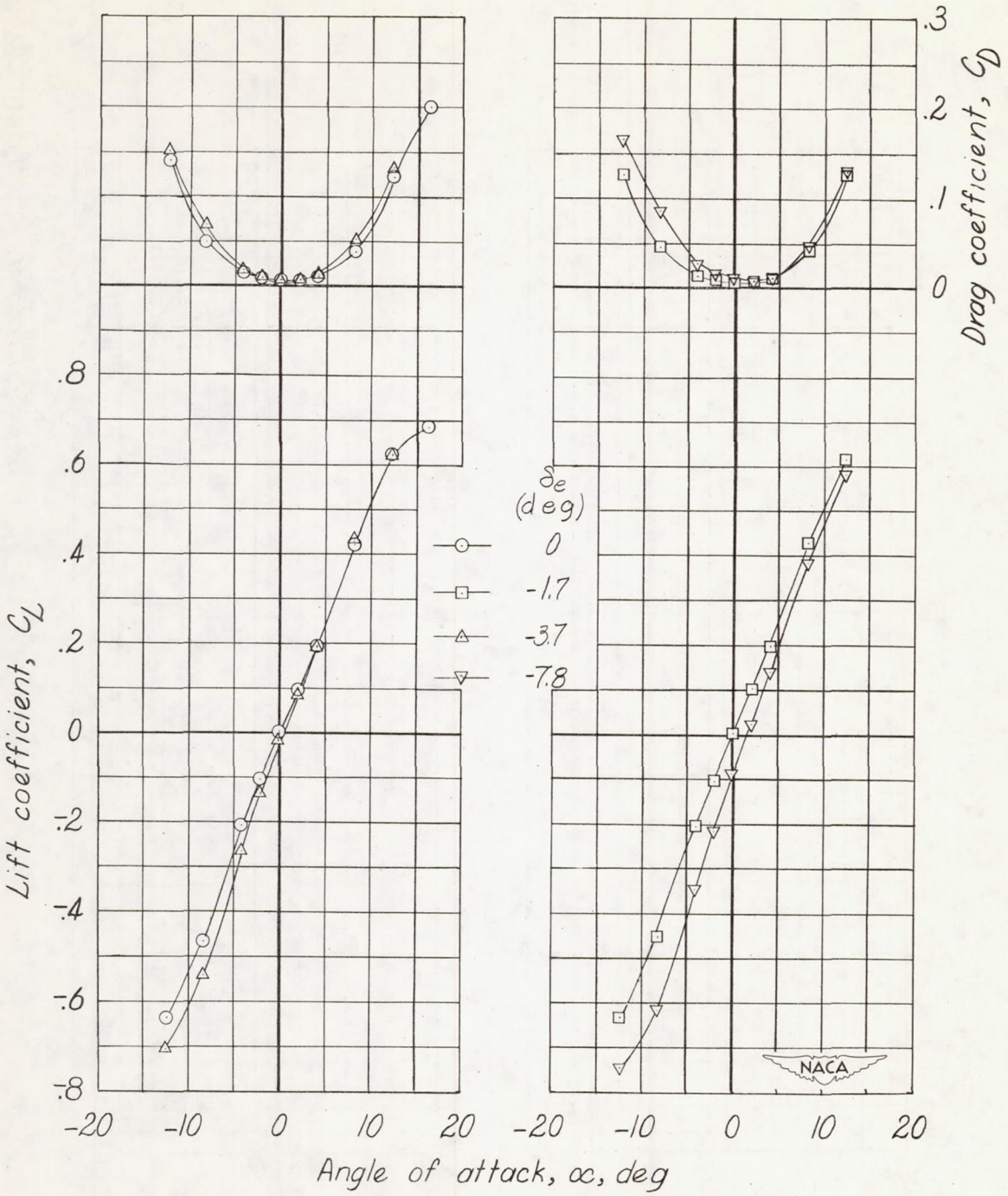


Figure 8.- Aerodynamic characteristics of the 45° sweptback horizontal-tail model equipped with the small faired horn. M = 0.86.

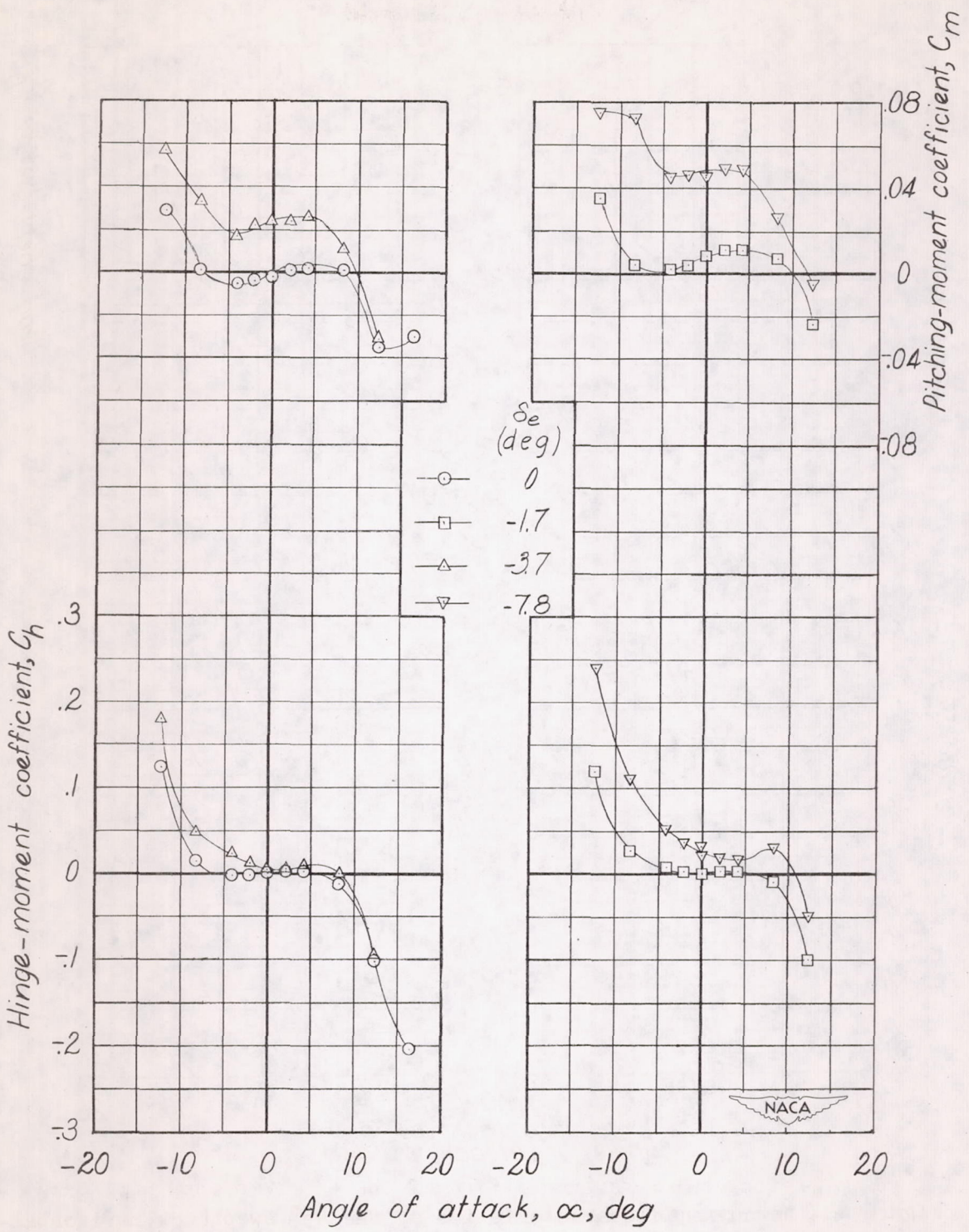


Figure 8.- Concluded.

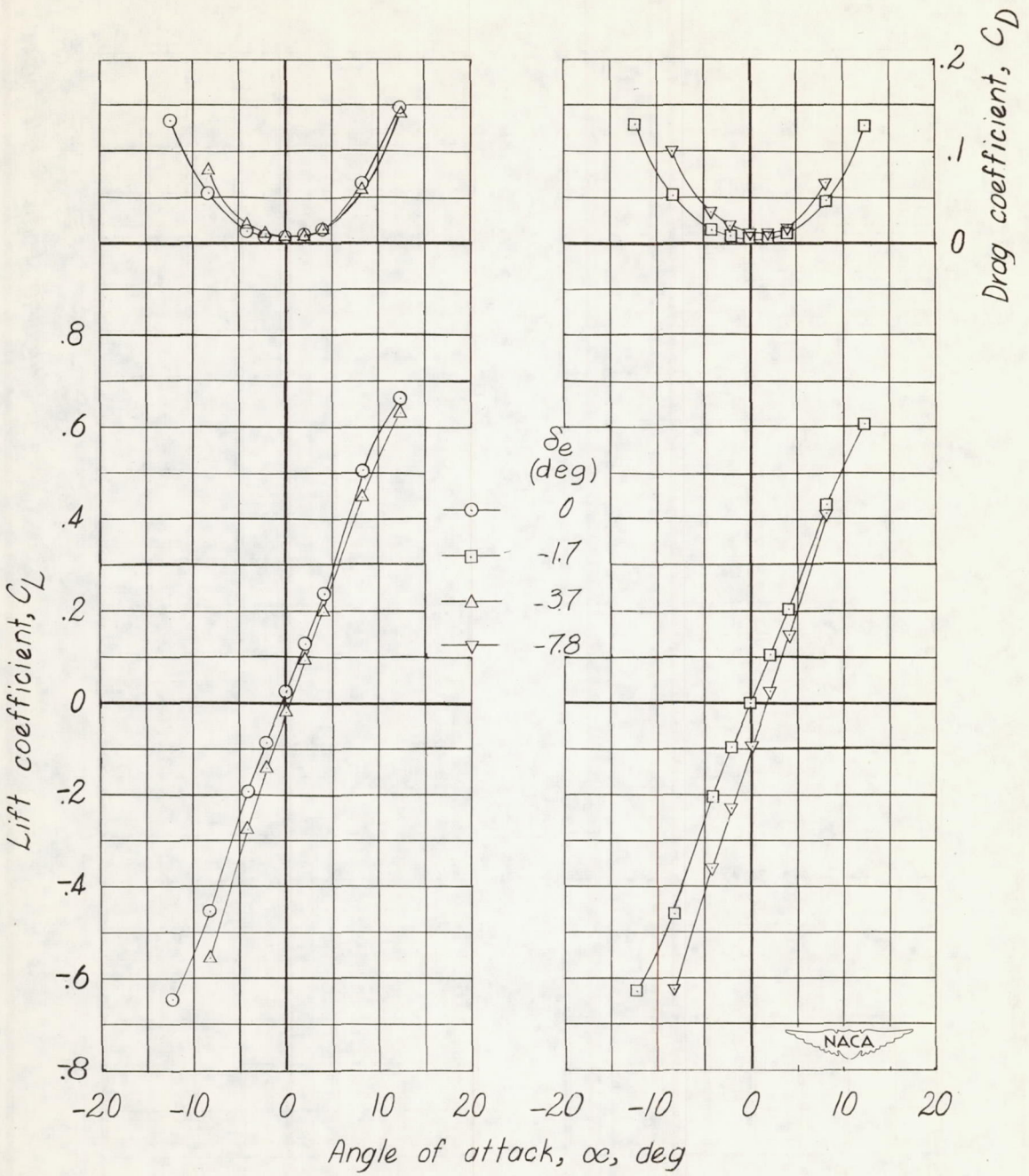


Figure 9.- Aerodynamic characteristics of the 45° sweptback horizontal-tail model equipped with the small faired horn. M = 0.88.

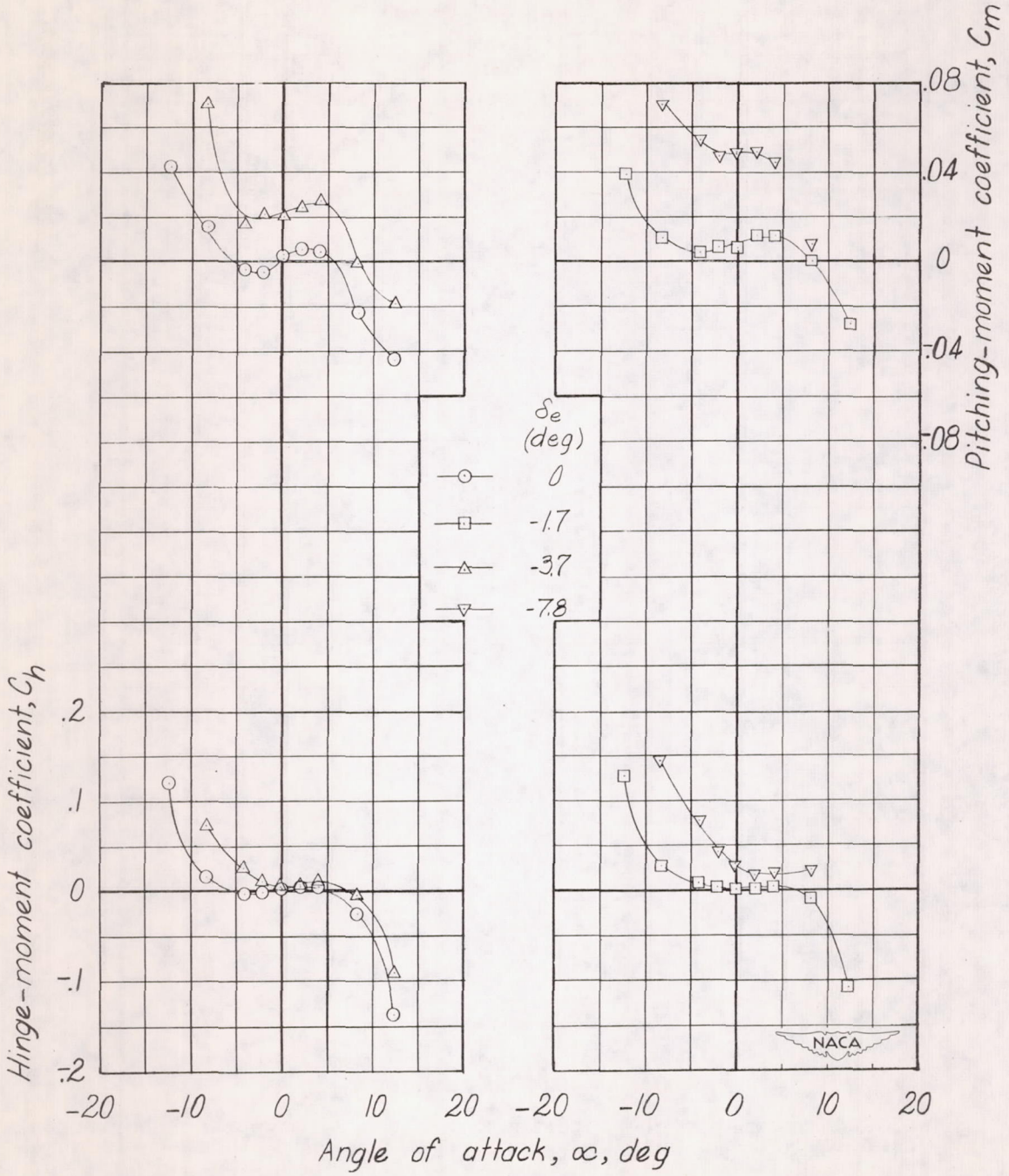


Figure 9.- Concluded.

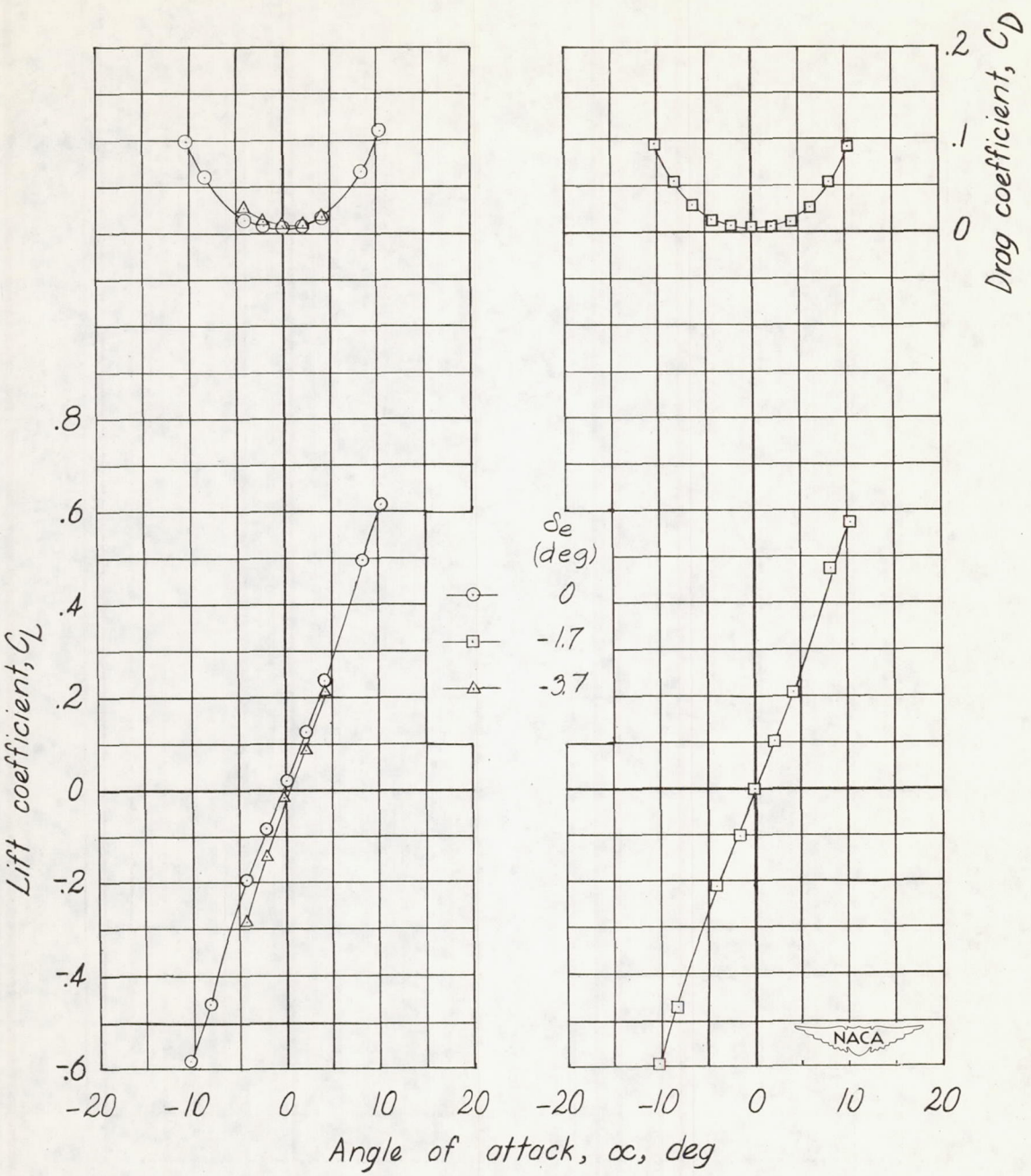


Figure 10.- Aerodynamic characteristics of the 45° sweptback horizontal-tail model equipped with the small faired horn. M = 0.90.

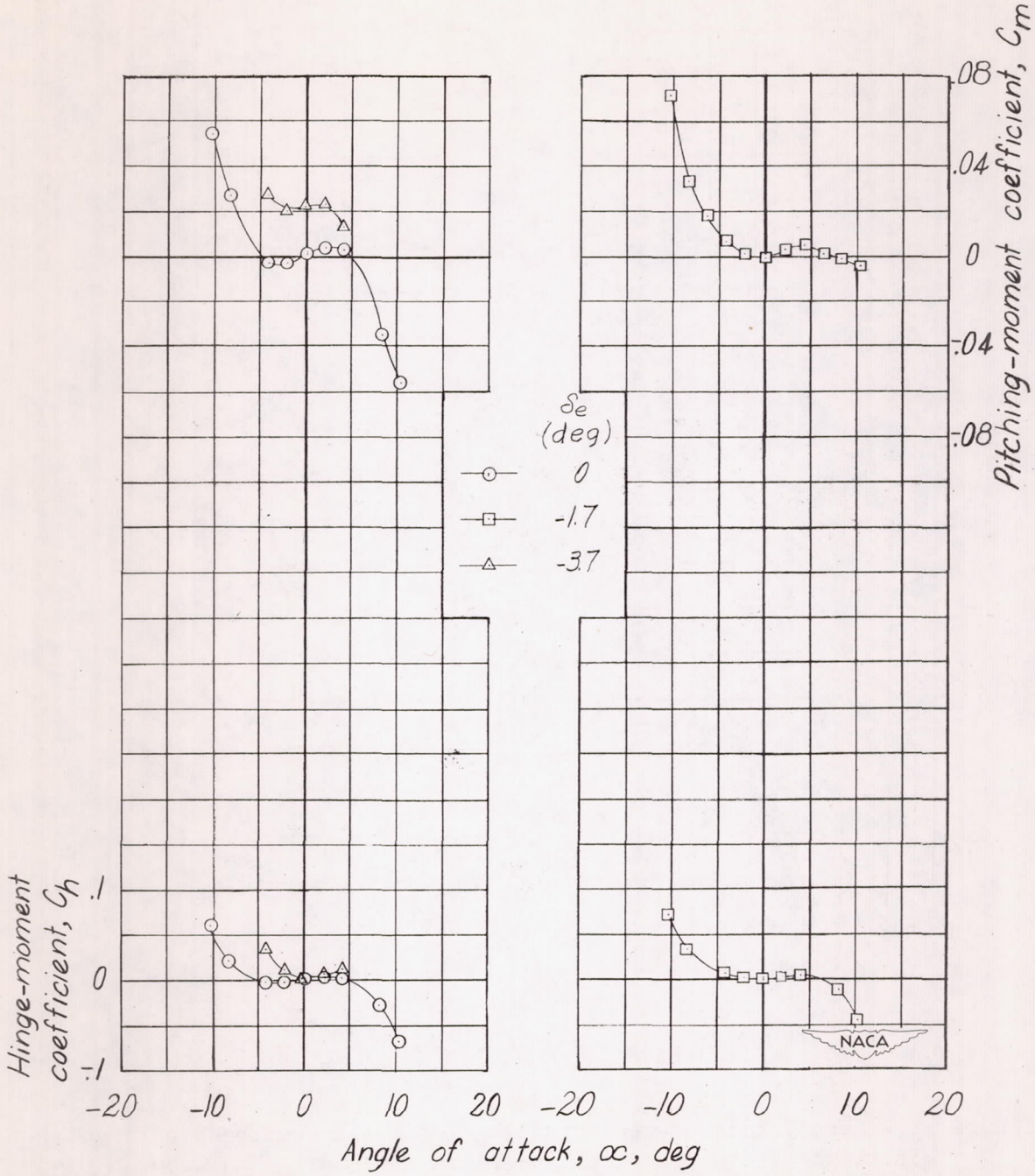


Figure 10.- Concluded.

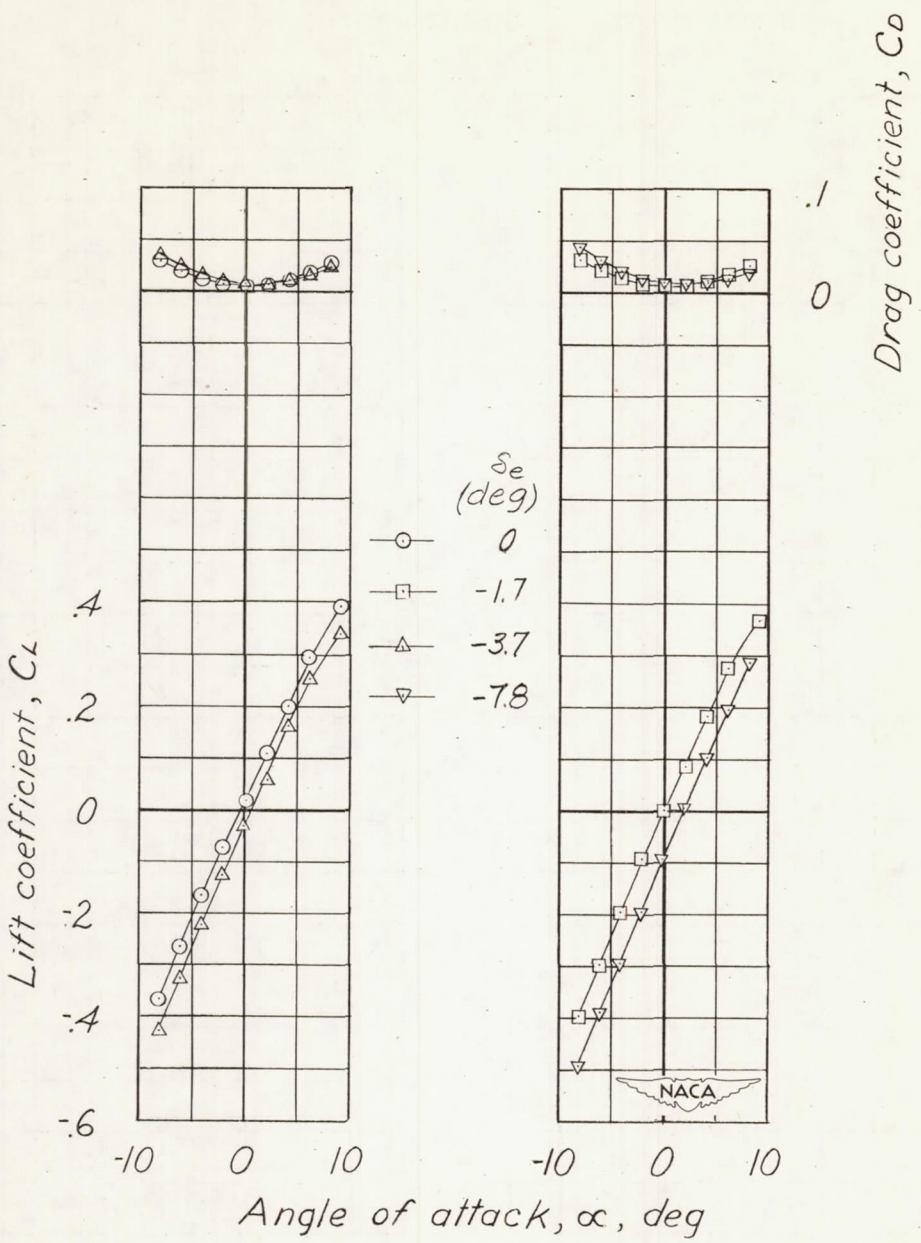


Figure 11.- Aerodynamic characteristics of the 45° sweptback horizontal-tail model equipped with the plain elevator. M = 0.50.

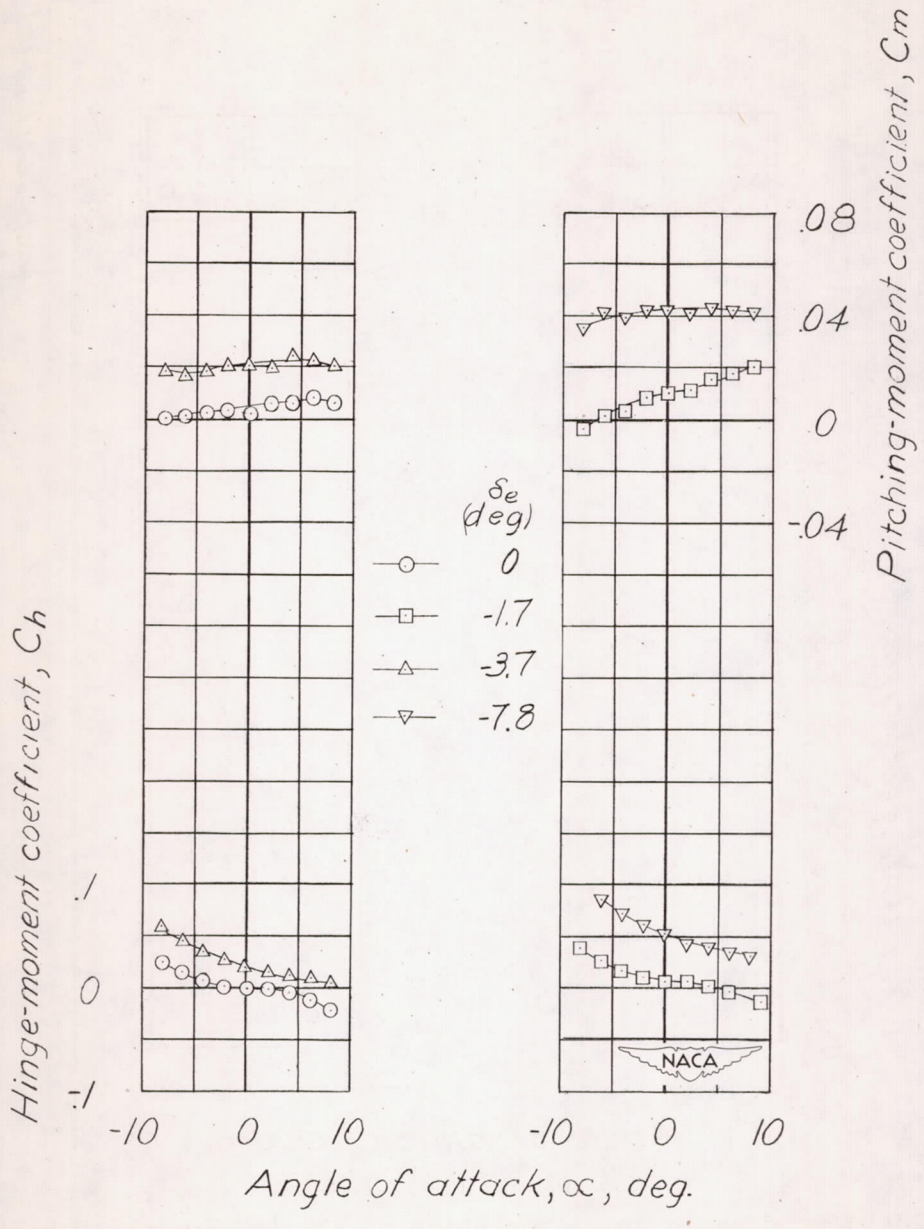


Figure 11.- Concluded.

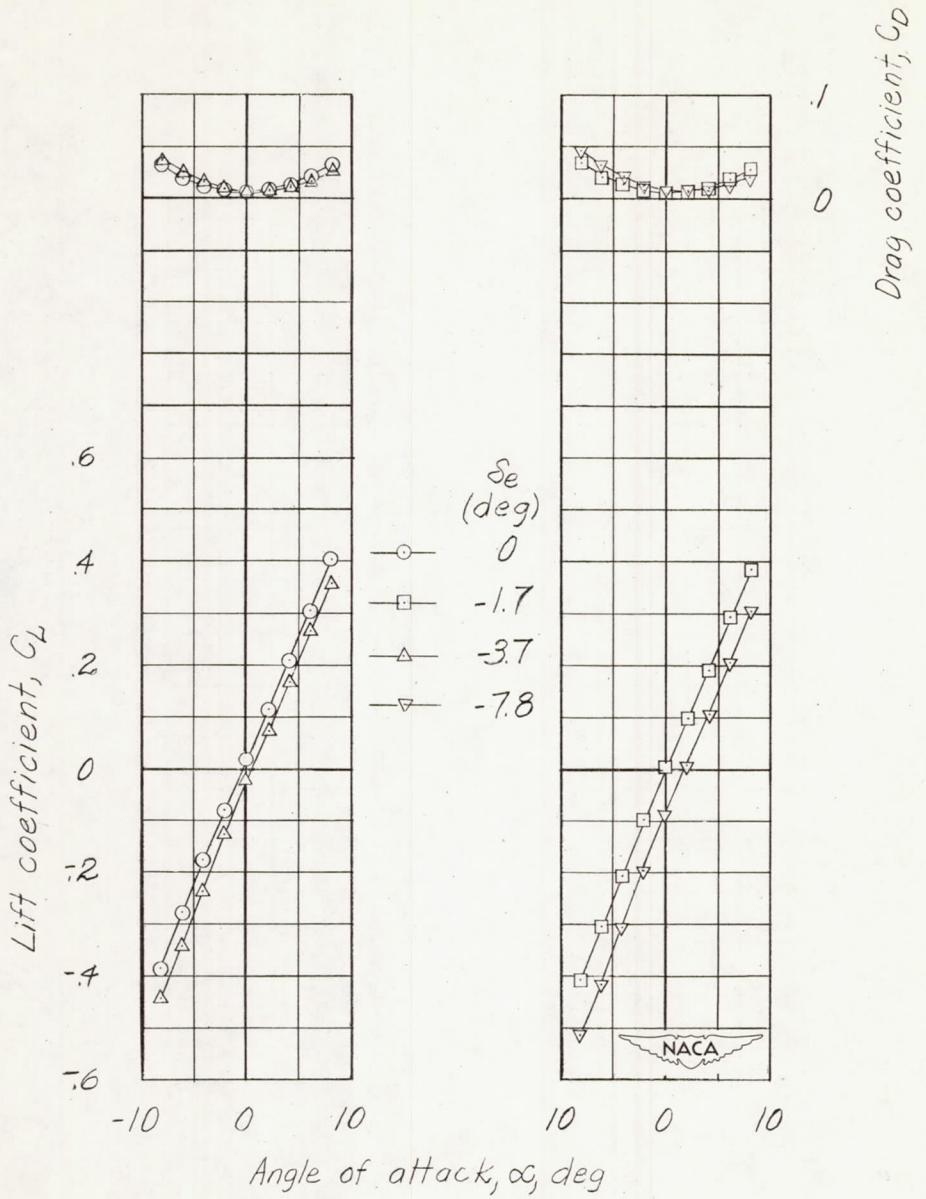


Figure 12.- Aerodynamic characteristics of the 45° sweptback horizontal-tail model equipped with the plain elevator. M = 0.70.

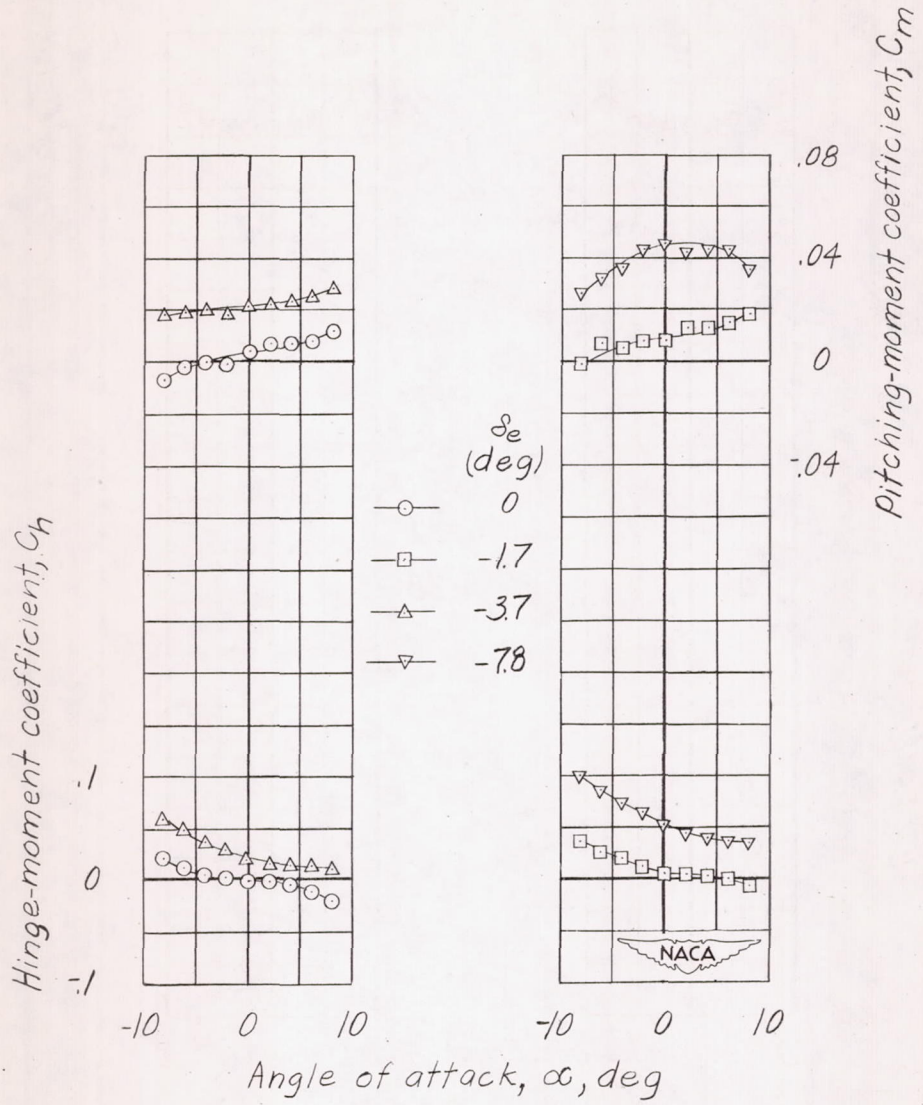


Figure 12.- Concluded.

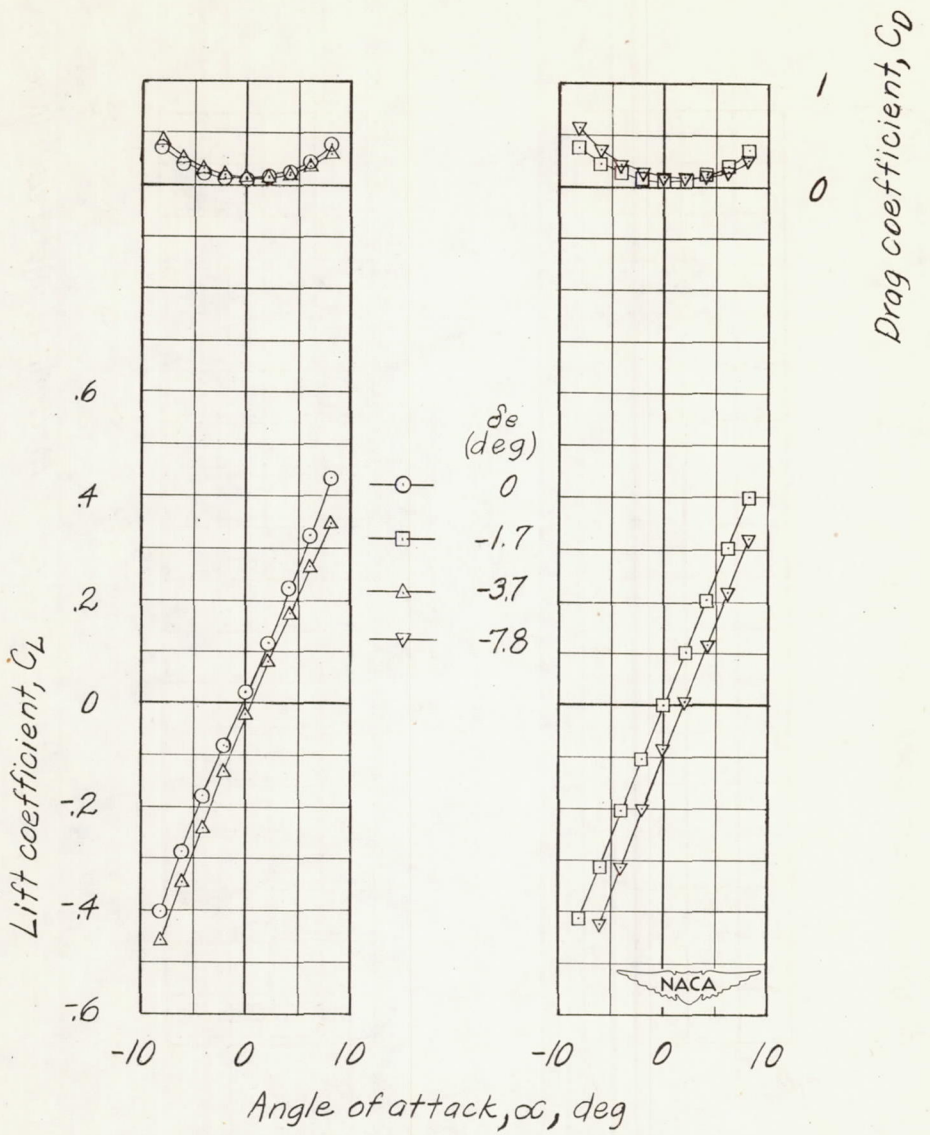


Figure 13.- Aerodynamic characteristics of the 45° sweptback horizontal-tail model equipped with the plain elevator. M = 0.80.

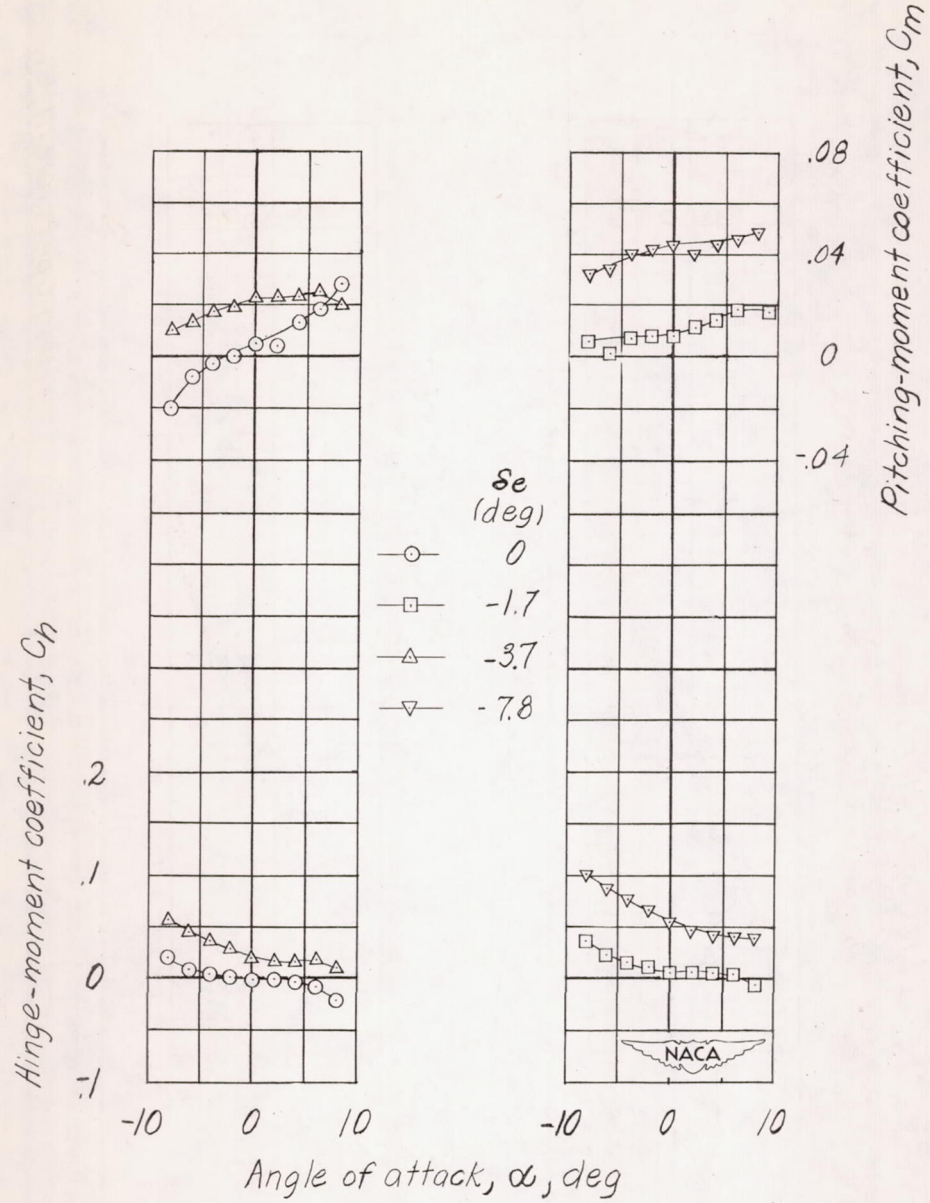


Figure 13.- Concluded.

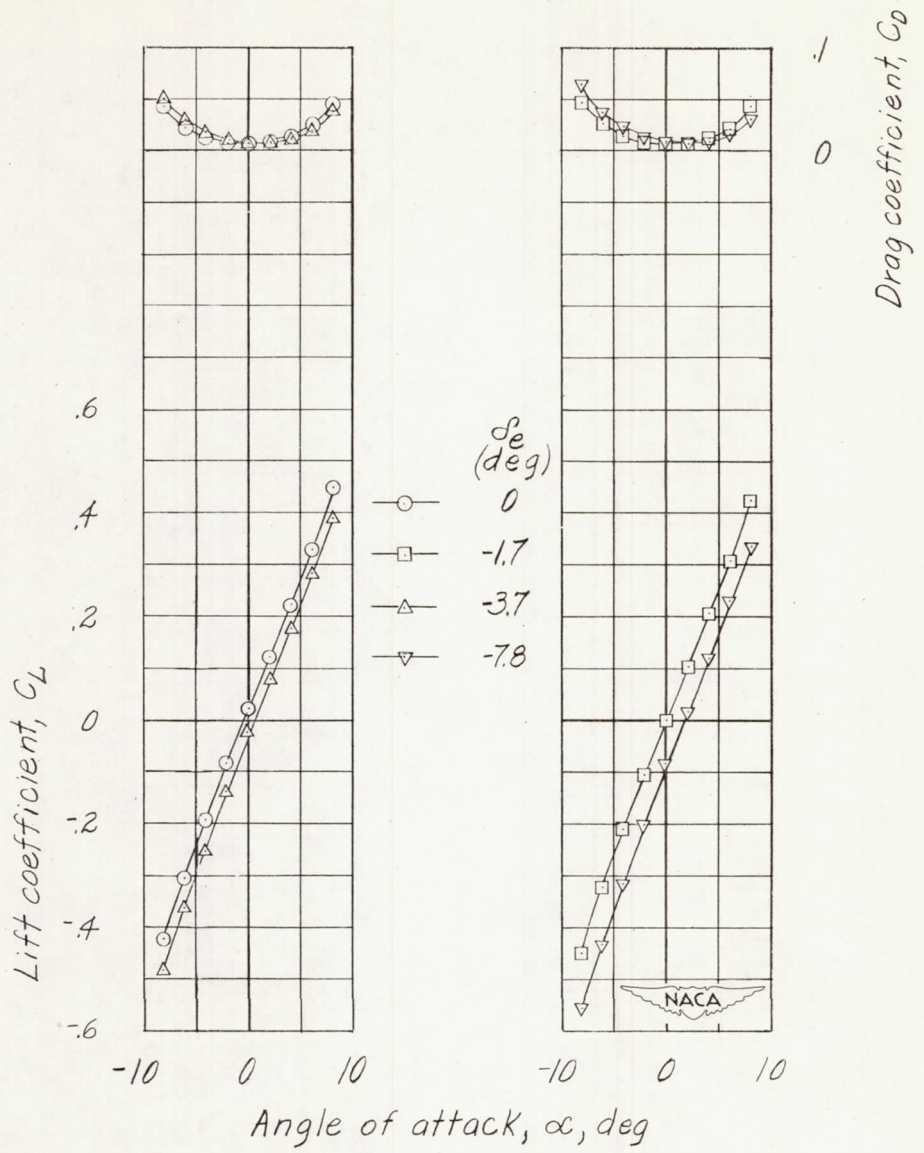


Figure 14.- Aerodynamic characteristics of the 45° sweptback horizontal-tail model equipped with the plain elevator. M = 0.84.

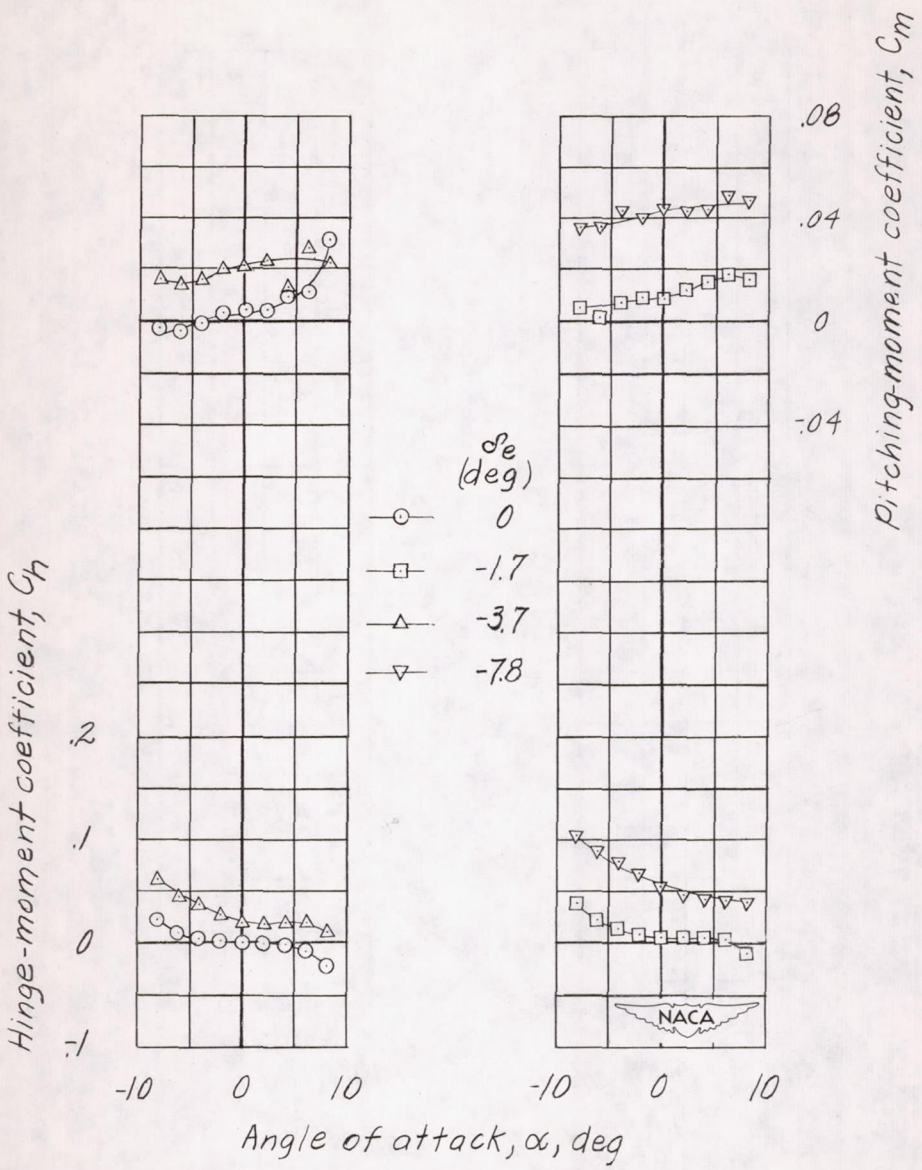


Figure 14.- Concluded.

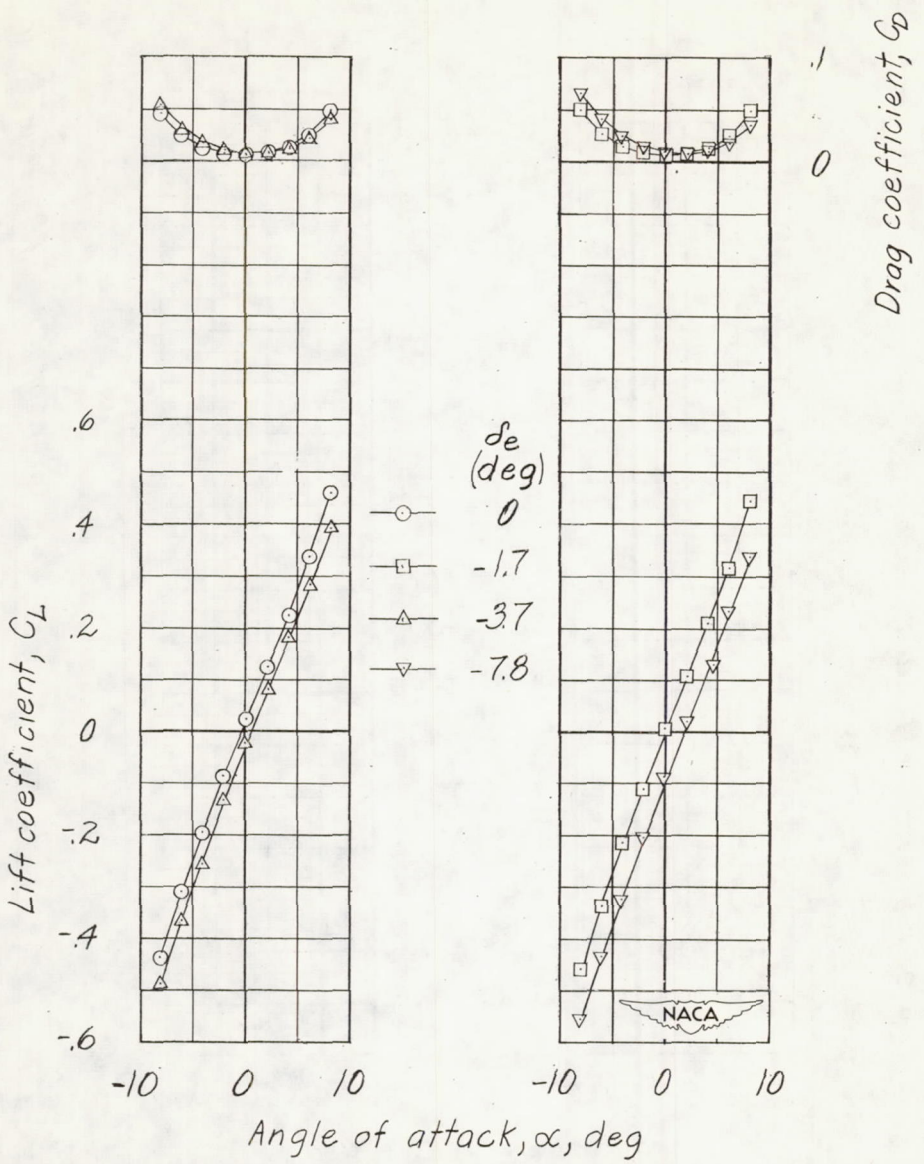


Figure 15.- Aerodynamic characteristics of the 45° sweptback horizontal-tail model equipped with the plain elevator. M = 0.86.

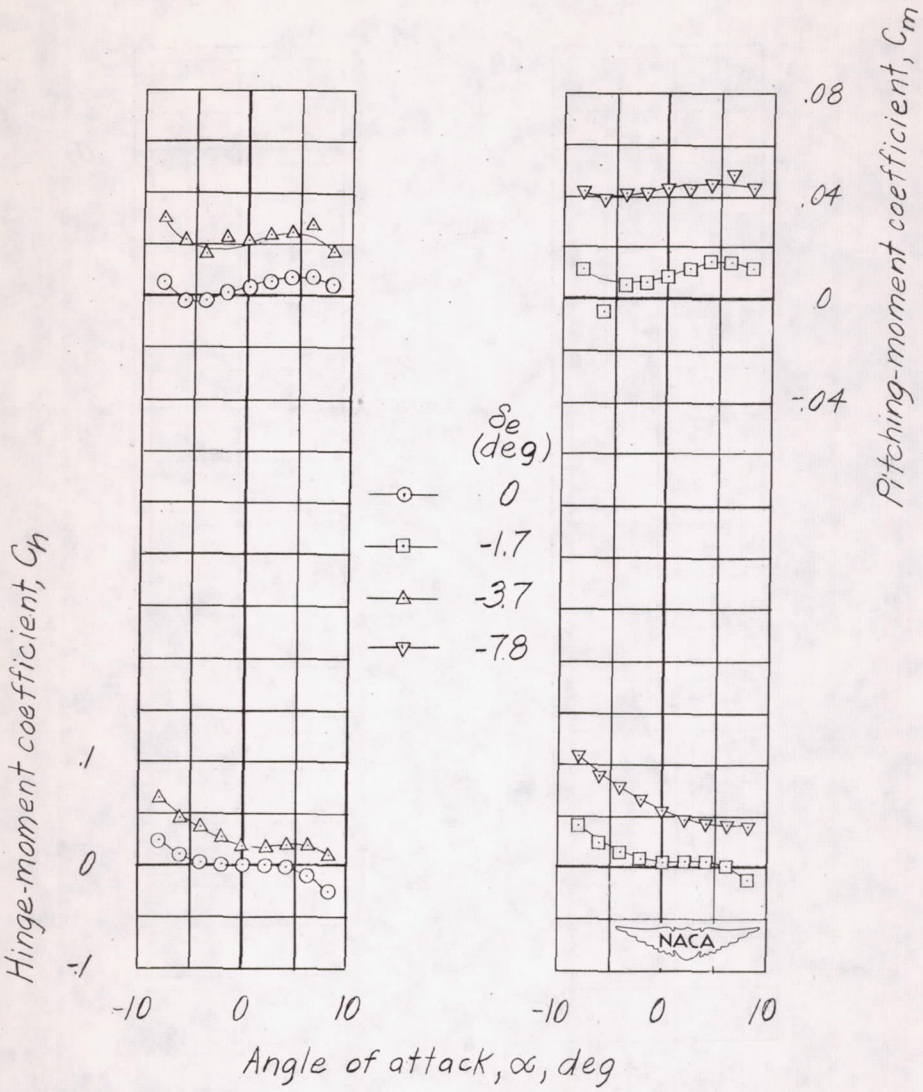


Figure 15.- Concluded.

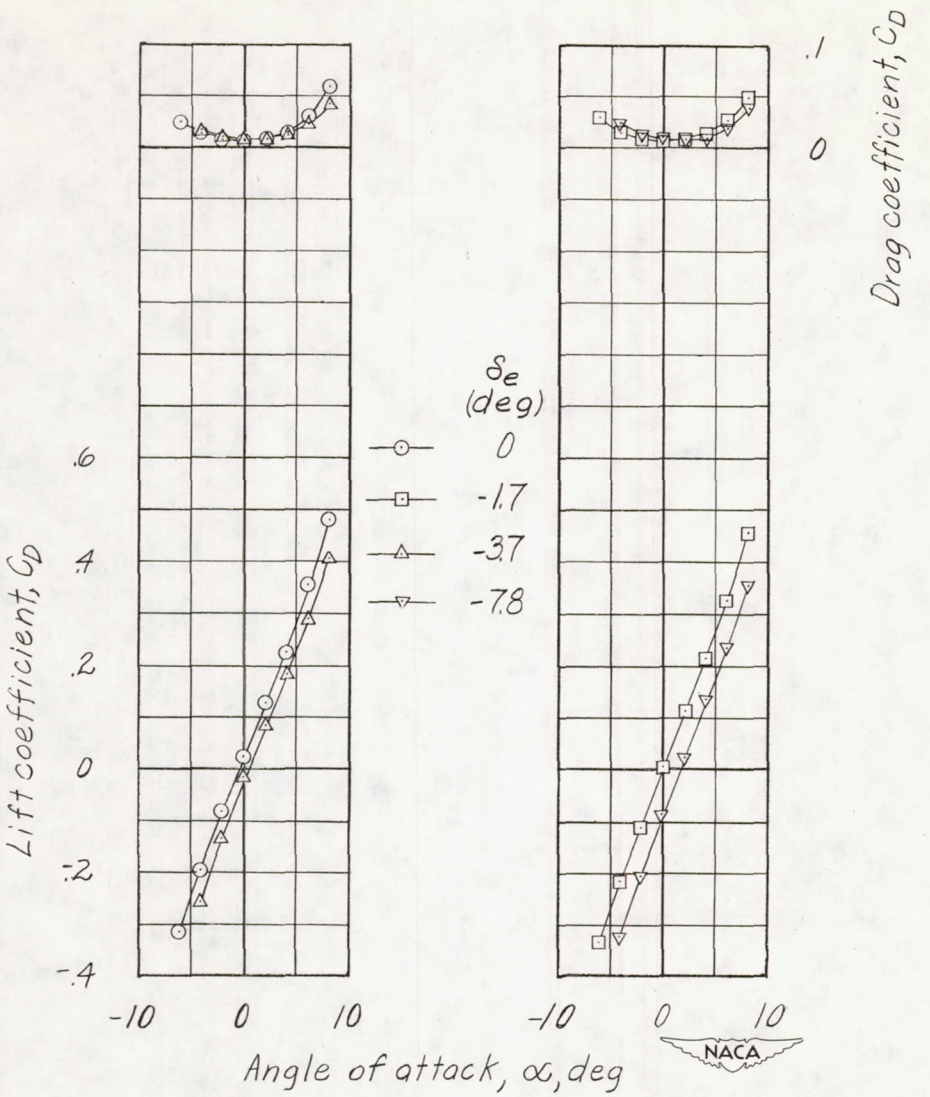


Figure 16.- Aerodynamic characteristics of the 45° sweptback horizontal-tail model equipped with the plain elevator. M = 0.89.

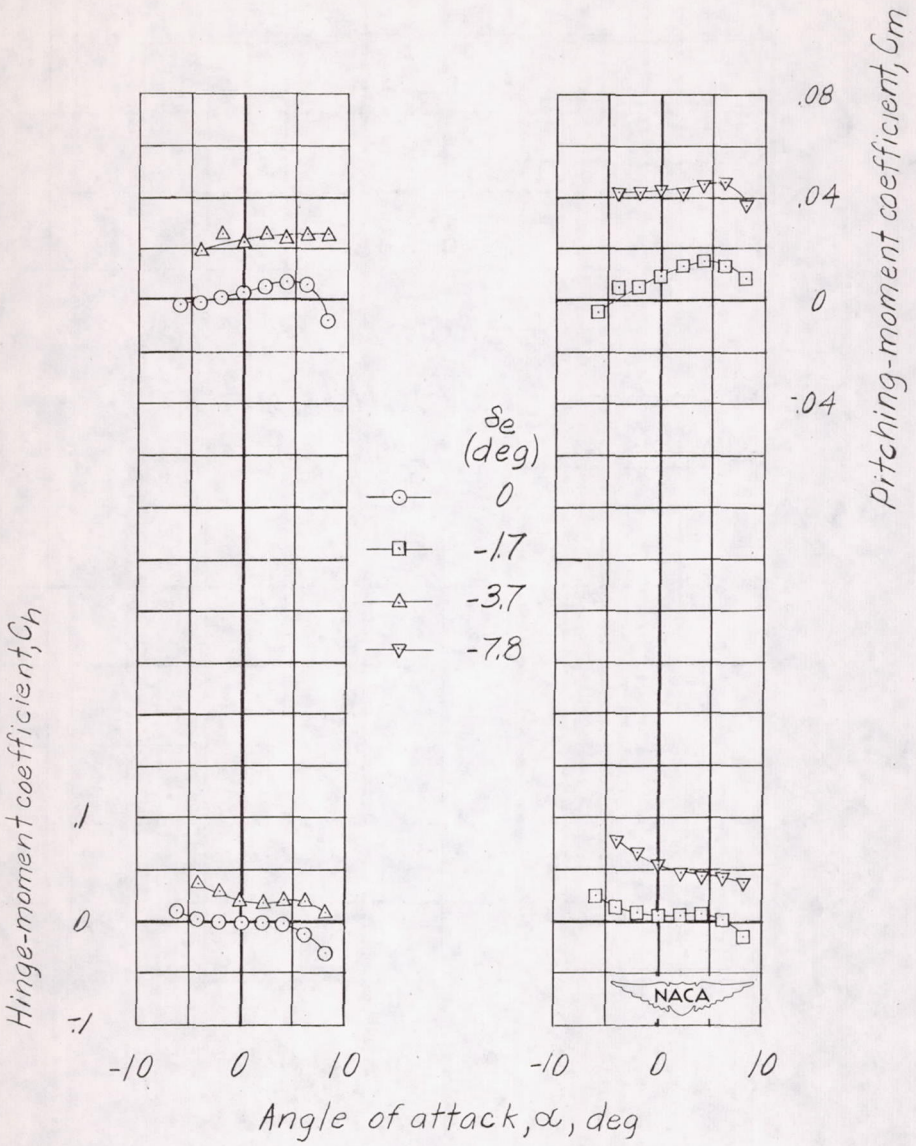


Figure 16.- Concluded.

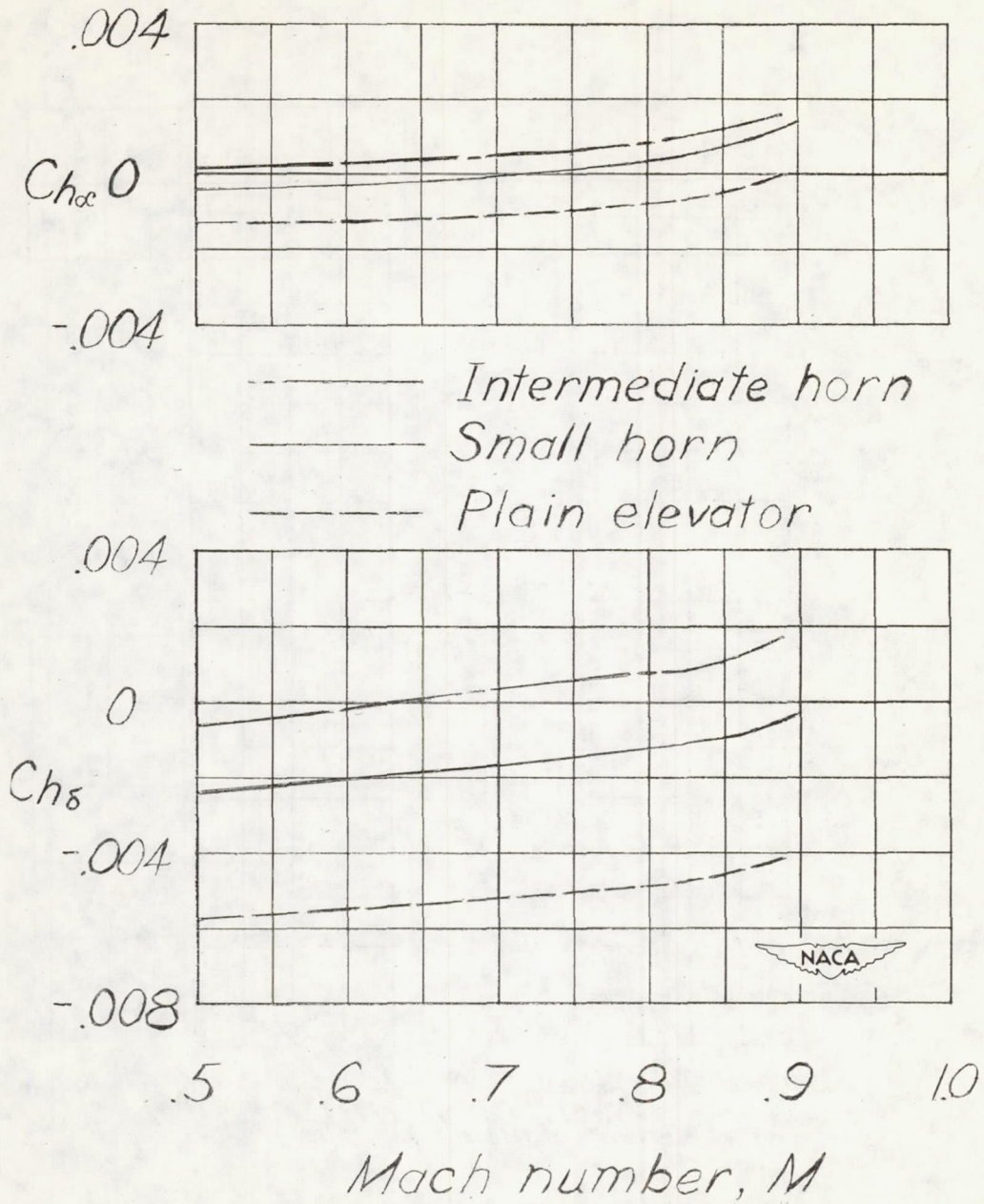


Figure 17.- Effect of Mach number on the hinge-moment parameters.

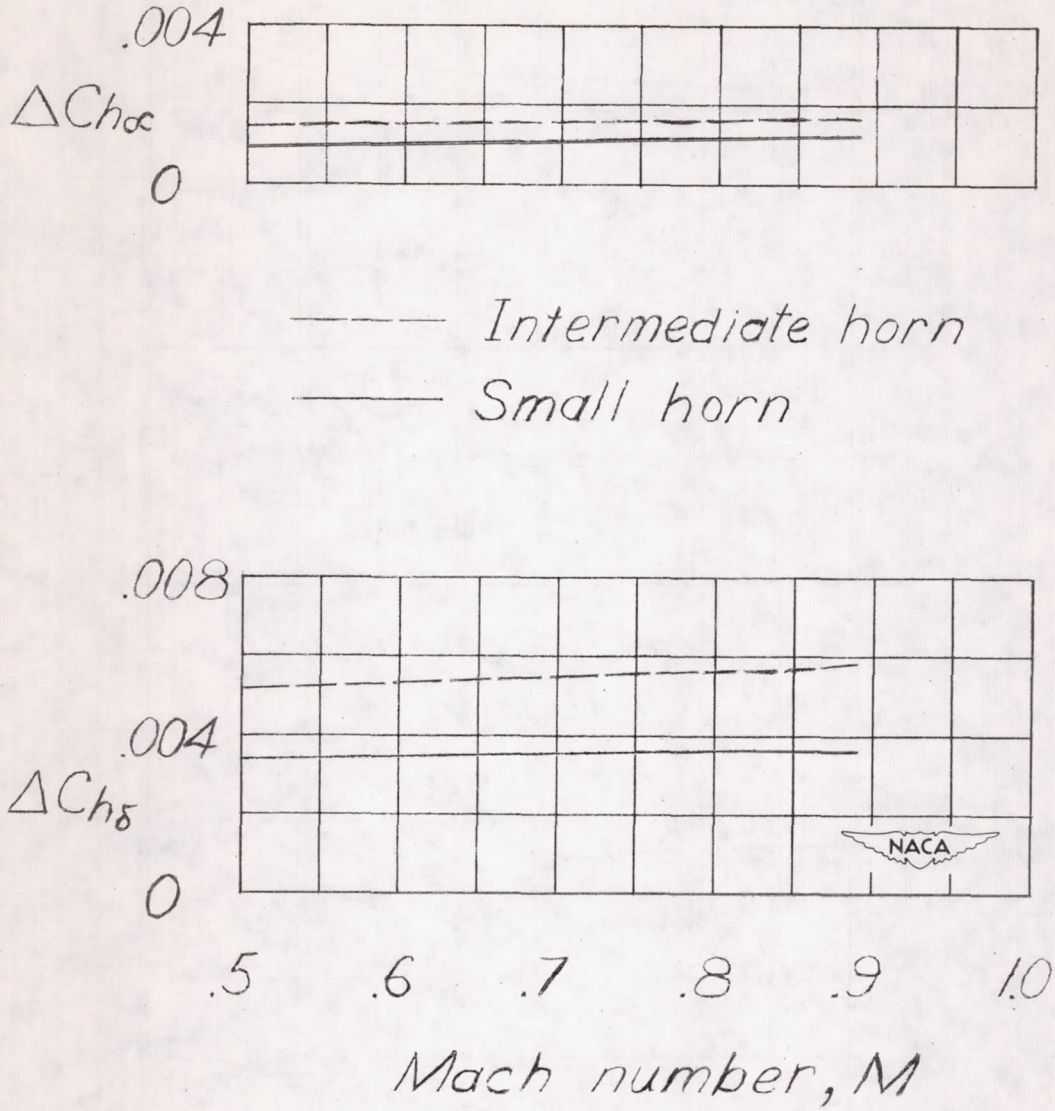


Figure 18.- Increments of hinge-moment parameters due to addition of horn balance to unbalanced elevator.

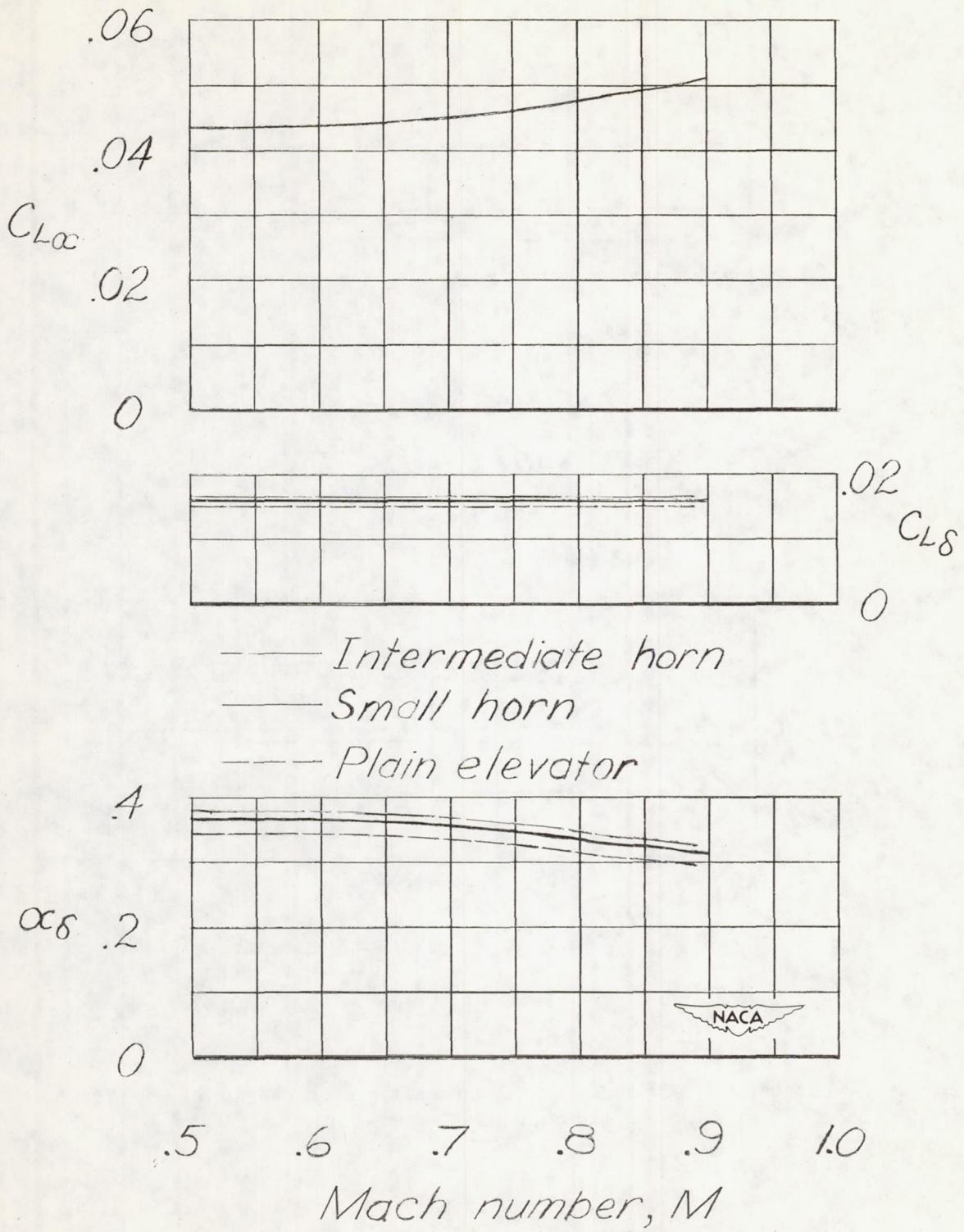


Figure 19.- Effects of Mach number on the lift parameters.